UNIVERSITY OF BIRMINGHAM

Relative skull size evolution in Mesozoic archosauromorphs

Bestwick, Jordan; Godoy, Pedro; Maidment, Susannah; Ezcurra, Martin; Wroe, Mia; Raven, Thomas; Bonsor, Joseph; Butler, Richard

Relative skull size evolution in Mesozoic archosauromorphs: potential drivers and morphological uniqueness of erythrosuchid archosauriforms

by JORDAN BESTWICK[1]* (iD), PEDRO L. GODOY[2,3] (iD),
SUSANNAH C. R. MAIDMENT[1,4] (iD), MARTÍN D. EZCURRA[1,5] (iD), MIA WROE[1],
THOMAS J. RAVEN[4,6] (iD), JOSEPH A. BONSOR[4,7] (iD) *and* RICHARD J. BUTLER[1] (iD)

[1]School of Geography, Earth and Environmental Sciences, University of Birmingham, Edgbaston, Birmingham, B15 2TT, UK; jordan.bestwick92@gmail.com
[2]Department of Zoology, Federal University of Paraná, 81531–980, Curitiba, Brazil
[3]Department of Anatomical Sciences, Stony Brook University, Stony Brook, NY 11794, USA
[4]Department of Earth Sciences, Natural History Museum, London, SW7 5DB, UK
[5]Sección Paleontolgía de Vertebrados, CONICET – Museo Argentino de Ciencias Naturales 'Bernardino Rivadavia', Ángel Gallardo 470 (C1405DJR), Buenos Aires, Argentina
[6]School of Environment and Technology, University of Brighton, Lewes Road, Brighton, BN1 4JG, UK
[7]Department of Biology and Biochemistry, University of Bath, Claverton Down, Bath, BA2 7AY, UK
*Corresponding author

Typescript received 12 October 2021; accepted in revised form 2 February 2022

Abstract: Little is known about the large-scale evolutionary patterns of skull size relative to body size, and the possible drivers behind these patterns, in Archosauromorpha. For example, the large skulls of erythrosuchids, a group of non-archosaurian archosauromorphs from the Early and Middle Triassic, and of theropod dinosaurs are regarded as convergent adaptations for hypercarnivory. However, few investigations have explicitly tested whether erythrosuchid and theropod skulls are indeed disproportionately large for their body size, and whether this trend is driven by hypercarnivory. Here, we investigate archosauromorph relative skull size evolution, examining the scaling relationships between skull and body size of Palaeozoic and Mesozoic archosauromorphs using a robust phylogenetic framework and assessing the influence of potential drivers, such as taxonomy, diet, locomotory mode and inhabited biotope. Our results show that archosauromorph relative skull sizes are largely determined by phylogeny and that the other drivers have much weaker levels of influence. We find negative allometric scaling of skull size with respect to body size when all studied archosauromorphs are analysed. Within specific groups, skull size scales with positive allometry in non-archosaurian archosauromorphs and, interestingly, scales isometrically in theropods. Ancestral reconstructions of skull–femur size ratio reveal a disproportionately large skull at the base of Erythrosuchidae and proportionately sized skulls at the bases of Theropoda, Carnosauria and Tyrannosauroidea. Relative skull sizes of erythrosuchids and theropods are therefore distinct from each other, indicating that disproportionately large skulls are not a prerequisite for hypercarnivory in archosauromorphs, and that erythrosuchids exhibit a bauplan unique among terrestrial Mesozoic carnivores.

Key words: relative skull size, Archosauromorpha, hypercarnivory, biotope, phylogeny, allometry.

THE vertebrate head is a remarkable anatomical structure with a diverse array of functions. These include but are not limited to: feeding; housing and protecting the brain; sensing and interpreting external cues; display; and intra- and inter-specific aggression (Stephens *et al.* 2007; Openshaw & Keogh 2014; VanBuren *et al.* 2015; da Silva *et al.* 2018; Arbour *et al.* 2019). Head phenotypes are therefore the outcome of numerous selective pressures (Bright *et al.* 2016). Currently, our understanding of whether selective pressures have additive, interactive or constraining effects on head phenotypes is still incomplete (Watanabe *et al.* 2019; Felice *et al.* 2021). For example, skull size relative to the rest of the body is often hypothesized to be influenced by diet; disproportionately larger skulls showing positive allometric scaling are suggested as an adaptation for hypercarnivory in many lineages (Figueirido *et al.* 2010; Butler *et al.* 2019; Galatius *et al.* 2020). However, such hypotheses often fail to account for other drivers that may concurrently influence skull size. Characterizing phenotypic changes such as relative skull size over evolutionary time within a rigorous phylogenetic context, as well as understanding the role of potential drivers (e.g. diet, inhabited biotope and mode of locomotion) are crucial for understanding the origins and radiations of past

and present biodiversity (VanBuren *et al.* 2015; Benson *et al.* 2018).

Archosauromorpha represents an excellent group for studying large-scale evolutionary patterns and possible drivers of relative skull size. This highly successful clade includes archosaurs (dinosaurs, birds, pterosaurs and crocodilians) and their close relatives, and is represented today by over 10 000 bird and around 27 crocodilian species (Brusatte *et al.* 2010*a*; Nesbitt 2011; Grigg & Kirshner 2015; Ezcurra & Butler 2018; Ezcurra *et al.* 2020*a*). Archosauromorphs evolved in the middle–late Permian and rapidly diversified in the wake of the Permo-Triassic mass extinction to dominate terrestrial ecosystems for almost the entirety of the Mesozoic (Benton 2004; Langer *et al.* 2010; Nesbitt 2011; Foth *et al.* 2016*a*, 2021; Ezcurra & Butler 2018). Lineages from this clade have also repeatedly radiated into other biotopes, with pterosaurs and birds (and possibly a few non-avian theropod maniraptoran dinosaurs) independently evolving active flight (Rayner 1988; Pei *et al.* 2020) and members of groups such as Crocodylomorpha, Phytosauria, Tanystropheidae and Proterosuchidae evolving semi or fully aquatic lifestyles (Stocker *et al.* 2017; Wilberg *et al.* 2019; Ezcurra *et al.* 2020*b*). In addition, today most major archosauromorph clades have well-resolved phylogenies that enable macroevolutionary investigations within robust phylogenetic frameworks (e.g. Ezcurra 2016; Benson *et al.* 2018; Godoy *et al.* 2019; O'Brien *et al.* 2019; Pradelli *et al.* 2021).

One pattern of particular interest concerns the repeated occupation of terrestrial hypercarnivorous niches (a diet comprising more than 70% meat; Holliday & Steppan 2004), by distantly related archosauromorphs throughout the Mesozoic. This niche is thought to have been occupied in the Early and Middle Triassic by erythrosuchids, a non-archosaurian archosauromorph clade of quadrupeds characterized by large skulls with a subrectangular profile (e.g. Butler *et al.* 2019; Ezcurra *et al.* 2020*b*, 2021; Maidment *et al.* 2020). Middle and Late Triassic hypercarnivorous niches are thought to have been filled by noncrocodylomorph loricatans (pseudosuchian archosaurs traditionally referred to as 'rauisuchians' *sensu* Nesbitt & Desojo 2017) which probably assumed both quadrupedal and bipedal postures (e.g. *Prestosuchus chinquensis* and *Postosuchus kirkpatricki* respectively; Chatterjee 1985; Weinbaum 2011, 2013; Mastrantonio *et al.* 2019; Desojo *et al.* 2020*a*). Multiple groups of theropod dinosaurs are regarded as the apex predators of Jurassic and Cretaceous food webs, such as megalosaurids in the former period and abelisaurids and tyrannosaurids in the latter (Therrien & Henderson 2007; Brusatte *et al.* 2012; Novas *et al.* 2013; Hendrickx & Mateus 2014). The large skulls exhibited by these archosauromorph groups are therefore deemed to be convergent adaptations for hypercarnivory (Chatterjee 1985; Nesbitt *et al.* 2013; Butler *et al.* 2019;

Ezcurra *et al.* 2021). However, the hypothesis that their skulls are indeed disproportionately large with respect to body size, and are also convergent with each other, has currently received little explicit testing (Therrien & Henderson 2007; Butler *et al.* 2019).

In this study, we investigate relative skull sizes of Palaeozoic and Mesozoic archosauromorphs to: (1) understand the influence of potential drivers (taxonomy, diet, locomotion and biotope) on relative skull size; (2) understand scaling relationships between skull and body size according to these potential drivers; and (3) reconstruct relative skull size evolution across Archosauromorpha. We achieve these aims using a robust phylogenetic framework that includes the construction of a novel informal supertree that is independently time-scaled using two distinct methods. This also enables better identification of whether relative skull size evolution, at both higher-level and more exclusive clades, is constant and directional, or indicates evolutionary radiations (i.e. increase in morphological diversity at the base of major clades) followed by stasis. Our study represents the first comprehensive investigation of large-scale patterns of skull size evolution across the Palaeozoic and Mesozoic in archosauromorphs.

MATERIAL AND METHOD

Skull and body size data collection

We collected data on basal skull length (anterior tip of the premaxilla to the posterior tip of the quadrate) and femur length across Palaeozoic and Mesozoic archosauromorphs. Skull length was our chosen proxy for skull size due to the ease of data collection on account of not relying on homologous landmarks between distantly related taxa, and due to its previous use in investigating cranial morphological disparity in extant archosaurs (Erickson *et al.* 2012; Foth *et al.* 2015; Shatkovska & Ghazali 2021). Femoral length was our chosen proxy for overall body size because while femur circumference scales more closely with body mass (Campione & Evans 2012; Campione *et al.* 2014; Maidment *et al.* 2020), femur length is also a reliable proxy for body mass that has been used extensively, is much easier to measure, and is much more widely reported than femur circumference in the literature (Carrano 2006; Sookias *et al.* 2012; Turner & Nesbitt 2013; VanBuren *et al.* 2015; Butler *et al.* 2019). Data were collected for a total of 223 species of archosauromorphs, 81 of which were drawn from Butler *et al.* (2019; and references therein). We added data from personal observations and the literature for a further 142 species, including non-archosaurian archosauromorphs, pseudosuchians, dinosaurs and pterosaurs. The characteristic parietosquamosal frills of ceratopsian dinosaurs

(e.g. *Triceratops horridus*) were not included in skull length measurements, in order to allow representative comparisons with non-ceratopsians (VanBuren *et al.* 2015). All data were log-transformed prior to analysis. For each species, skull and femur data were acquired from a single individual in order to provide a representative ratio. This specimen was the largest best-preserved individual of that taxon to minimize any confounding effects from ontogeny, because ontogenetic trajectories of cranial shape from several groups of extant and extinct archosaurs (such as crocodilians and dinosaurs respectively) show crania generally become more elongate with increasing ontogenetic stage (Foth *et al.* 2016*b*; Morris *et al.* 2019; Lee *et al.* 2020; Fabbri *et al.* 2021). The relative ontogenetic stage was considered for all study specimens, either from prior assessments where data were obtained from the literature, or by morphological assessments where data were collected from personal observations, including the size and degree of bone and sutural fusion. Specimens assessed as potential hatchlings or juveniles were not sampled. The full list of studied archosauromorphs, including skull and femur measurements and data sources, can be found in Table S1.

Building the archosauromorph supertree

To explore our data in a robust phylogenetic framework, we created an informal supertree for all sampled archosauromorphs. The supertree comprises 1307 species-level taxa and was built using the topology used by Butler *et al.* (2019; and references therein) with input from: a modified version of Ezcurra (2016) for non-archosaurian archosauromorphs and non-crocodylomorph pseudosuchians; Ezcurra *et al.* (2020*a*) for non-pterosaur pterosauromorphs; Godoy *et al.* (2019) for crocodylomorphs; Andres *et al.* (2014) and Longrich *et al.* (2018) for Pterosauria; Raven & Maidment (2017) for Stegosauria; Rivera-Sylva *et al.* (2018) for Ankylosauria; Williamson & Brusatte (2016) for Pachycephalosauria; VanBuren *et al.* (2015) for Ceratopsia; Xing & Xing (2014) and McDonald *et al.* (2017) for Ornithopoda; Cashmore *et al.* (2020; and references therein) for Sauropodomorpha; Pol & Rauhut (2012) and Wang *et al.* (2017) for Ceratosauria; Rauhut & Pol (2019) for Carnosauria; Delcourt & Grillo (2018) for Tyrannosauroidea; Lee *et al.* (2014*a*) for Ornithomimosauria; Hartman *et al.* (2019) for Therizinosauria; Xu *et al.* (2010) for Alvarezsauroidea; Lamanna *et al.* (2014) and Funston *et al.* (2018) for Oviraptorosauria and; Pei *et al.* (2020) for Paraves. The complete tree can be found in Appendix S1. Stratigraphic ages for species were taken either from the literature or from the Paleobiology Database (https://paleobiodb.org) and can be found in Table S2. The supertree was time-scaled

using two different approaches to facilitate robust investigations into relative skull size evolution. We used the minimum branch length (*mbl*) method (Laurin 2004) with the minimum branch duration set at 1 myr (hereafter *mbl*.1) and the *cal3* method (Bapst 2013). The two time-scaling approaches were applied using functions *timePaleoPhy* and *cal3TimePaleoPhy* from the package *paleotree* (Bapst 2012) in R version 4.1.0 (R Core Team 2018). For the *cal3* method, the sampling rate was randomly drawn from a uniform distribution of previously estimated rates for tetrapods (Lloyd *et al.* 2016; Bapst & Hopkins 2017), whereas diversification and extinction rates (which we assume here to be the same) were obtained using the function *Rate2sProb* and dividing them by the interval length. Prior to time-scaling, we randomly resolved all polytomies in the supertree generating 20 different fully resolved trees, which, after time-scaling, resulted in 40 time-scaled trees (20 for each time-scaling approach). Analyses were performed using pruned versions of the *mbl*.1 and *cal3* trees that included only archosauromorphs for which we had collected skull and body size data. Example code used to perform all analyses in R can be found in Appendix S2.

Phylogenetic signal and potential drivers of skull size evolution

We tested for the presence of a phylogenetic signal in the ratio of skull length to femur length using the *phyloSignal* function of the package *phylosignal* (Keck *et al.* 2016), setting 999 999 replicates for each tree. We used Pagel's lambda (λ) as our index for testing phylogenetic signal as it is relatively robust when using trees with poorly resolved branch length information (Münkemüller *et al.* 2012; Molina-Venegas & Rodríguez 2017).

We applied regression models to examine the relationship between skull length and femur length in all archosauromorphs, and to investigate the effects of different drivers on this relationship. To take the phylogenetic relationships of taxa into account, we used phylogenetic generalized least squares (PGLS) regressions with the *gls* function from the package *nlme* (Pinheiro *et al.* 2018). We selected four predictors for our models: (1) taxonomy; (2) dietary group; (3) locomotory mode; and (4) inhabited biotope.

For taxonomy, archosauromorphs were assigned to one of the following clades or grades, some of which are modified from their formal phylogenetic definitions for easier between-group comparisons: (1) Avialae, the clade containing *Passer domesticus* and all coelurosaurian dinosaurs more closely related to it than to *Dromaeosaurus albertensis* and *Troodon formosus* (Turner *et al.* 2012); anchiornithines are included in this clade following Pei *et al.* (2020); (2) 'basal

archosauromorphs', a paraphyletic group that comprises all non-archosaurian archosauromorphs (including tanystropheids, rhynchosaurs, proterosuchids, erythrosuchids and proterochampsians; Ezcurra *et al.* 2020*b*), all non-crocodylomorph pseudosuchians (including phytosaurs, gracilisuchids, aetosaurs, ornithosuchids, erpetosuchids, poposauroids and non-crocodylomorph loricatans; Brusatte *et al.* 2010*a*; Nesbitt *et al.* 2013; Ezcurra 2016; Müller *et al.* 2020) and all non-dinosaurian and non-pterosaurian avemetatarsalians (e.g. *Scleromochlus taylori*); (3) Ceratopsia, the clade comprising all marginocephalian dinosaurs that are more closely related to *Triceratops horridus* than to *Pachycephalosaurus wyomingensis* (You & Dodson 2004); (4) Crocodylomorpha, the most inclusive clade containing *Crocodylus niloticus* but not *Rauisuchus tiradentes*, *Gracilisuchus stipanicicorum*, *Prestosuchus chiniquensis* or *Aetosaurus ferratus* (Nesbitt 2011; Irmis *et al.* 2013); (5) Dinosauria, the clade comprising the most recent common ancestor of *Triceratops horridus* and *Passer domesticus* and all its descendants (Brusatte *et al.* 2010*b*); Mesozoic avialans, however, are excluded from this category since their bauplans are adapted for flight; (6) basal Ornithischia, a paraphyletic group including all ornithischians that are not included within Ceratopsia, Ornithopoda or Thyreophora (e.g. *Heterodontosaurus tucki*); (7) Ornithopoda, the clade comprising all dinosaurs that are more closely related to *Edmontosaurus regalis* than to *Triceratops horridus* (Norman *et al.* 2004*a*); (8) Pterosauria, the clade comprising the most recent common ancestor of *Preondactylus buffarinii* and *Quetzalcoatlus northropi* and all its descendants (Nesbitt 2011); (9) Sauropodomorpha, the clade comprising all dinosaurs that are more closely related to *Saltasaurus loricatus* than to *Passer domesticus* (Galton & Upchurch 2004); (10) Theropoda, the largest clade containing *Allosaurus fragilis* but neither *Plateosaurus engelhardti* nor *Heterodontosaurus tucki* (Naish *et al.* 2020); members of Herrerasauria, all dinosaurs that share a more recent common ancestor with *Herrerasaurus ischigualastensis* than with *Liliensternus liliensterni* or *Plateosaurus engelhardti* (Langer 2004), are here included within Theropoda for simplicity despite growing evidence that this clade may represent non-theropod saurischians (Novas *et al.* 2021; and references therein); as with our Dinosauria clade, avialans are excluded from Theropoda here to rule out confounding effects from their highly derived bauplans; and (11) Thyreophora, the clade comprising all dinosaurs that are more closely related to *Ankylosaurus magniventris* than to *Triceratops horridus* (Norman *et al.* 2004*b*). Regression models were also performed on Archosauromorpha and Dinosauria with sauropodomorphs excluded to explore whether these dinosaurs had disproportionate effects on regression slopes due to their characteristically small skulls (Sander *et al.* 2010; Rauhut *et al.* 2011).

For diet, archosauromorphs were categorized as either carnivores or herbivores. This dichotomy is a simplification of the range of likely ecologies exhibited by extinct taxa but is necessary because of the difficulty in reliably assigning specific ecologies based on dietary proxies (see Bestwick *et al.* (2018) and Miller & Pittman (2021) for recent reviews) and allows straightforward analyses. For biotope, archosauromorphs were categorized as either terrestrial, aquatic (including semi-aquatic lifestyles) or aerial. For locomotion, archosauromorphs were categorized as either obligate bipeds, obligate quadrupeds, facultative biped-quadrupeds or bipedal-flying. All assignments for diet, locomotion and biotope were based on the common consensus of the literature and of the authors. We note that our aerial biotope and biped-flying categories have the same assigned taxa: avialans and pterosaurs and a few theropods (complete category assignments for all archosauromorphs can be found in Table S1).

A total of 15 models were used in our approach, including a no predictor model, single predictor models, and a model for a two, three and four-way combination of predictors. Each of the 15 models was fitted to all 40 trees. We initially performed a stepwise removal model to remove all non-significant interaction terms from our multi-predictor models. This resulted in all interaction terms being removed (i.e. all predictors were analysed as additive fixed factors). We compared the mean average and median AIC scores from each model to assess how well they explained our data.

Subsequent PGLS regressions were performed on each subset of the archosauromorph dataset according to taxonomy, diet, locomotory mode and biotope. To test the additional hypothesis that hypercarnivory is a driver behind large relative skull sizes, PGLS was also performed on terrestrial basal archosauromorph carnivores and terrestrial dinosaur carnivores. The non-crocodylomorph loricatans *Prestosuchus chinquensis* and *Postosuchus kirkpatricki* were included as part of the former carnivore subset due to the lack of sampled taxa from this group of Middle–Late Triassic predatory archosauromorphs. This, however, still enables comparisons between Triassic carnivores and Jurassic and Cretaceous carnivores. To reduce computational demands, all 'subset PGLS regressions' were performed using just one randomly chosen tree from each timescaling approach (i.e. one *mbl*.1 tree and one *cal3* tree).

Relative skull size evolution

To investigate relative skull size evolution in Archosauromorpha, one randomly chosen tree from each timescaling approach was pruned in R to include only archosauromorphs with sampled skull length and femur length data. Pruning has no effect on the topological relationships of remaining archosauromorphs. Ancestral reconstructions of log skull-length/log femur-length ratio

(henceforth: skull–femur ratio) were subsequently mapped onto each of the pruned supertrees. Maximum likelihood estimations were achieved using the *contMap* function in *phytools* (Revell 2012). In addition, to help determine whether ratio changes through evolutionary time are continuous or are better explained by evolutionary radiations (i.e. most significant shifts associated with the origin of major clades), we calculated ancestral skull–femur ratios along with variance and upper and lower 95% confidence intervals for 16 specific nodes (the same for each tree), using the *anc.ML* function in *phytools*. These nodes represent ratio estimates for the most recent common ancestor of a particular clade. For consistency with our PGLS and scaling analyses, nodes were selected to represent the following clades: Avialae, Ceratopsia, Crocodylomorpha, Dinosauria, basal Ornithischia, Ornithopoda, Pterosauria, Sauropodomorpha, Theropoda and Thyreophora. The taxonomic contents of these groups were not modified for this analysis. To further aid in identifying evolutionary changes we selected additional nodes that represented the following clades: Archosauromorpha (all saurians more closely to *Protorosaurus* than to Lepidosauria; Dilkes 1998), Archosauria (the least inclusive clade containing *Crocodylus niloticus* and *Passer domesticus*; Sereno 2005), Avemetatarsalia (the most inclusive clade containing *Passer domesticus* but not *Crocodylus niloticus*; Benton 1999), and Pseudosuchia (the most inclusive clade containing *Crocodylus niloticus* but not *Passer domesticus*; Sereno 2005). We also selected nodes that represented Erythrosuchidae (all taxa more closely related to *Erythrosuchus africanus* than to *Proterosuchus fergusi* or *Passer domesticus*; Ezcurra *et al.* 2010), Loricata (the most inclusive clade containing *Crocodylus niloticus* but not *Poposaurus gracilis*, *Ornithosuchus longidens* or *Aetosaurus ferratus*; Nesbitt 2011), Abelisauroidea (theropod dinosaurs more closely related to *Carnotaurus sastrei* than to *Ceratosaurus nasicornis*; Tykoski & Rowe 2004), Carnosauria (theropod dinosaurs more closely related to *Allosaurus fragilis* and to *Megalosaurus bucklandii* than to *Passer domesticus*; Rauhut & Pol 2019) and Tyrannosauroidea (all theropod dinosaurs more closely related to *Tyrannosaurus rex* than to *Ornithomimus velox*, *Deinonychus antirrhopus* or *Allosaurus fragilis*; Holtz 2004) to understand skull size evolution in unrelated apex predators from across the Mesozoic, and how they compare with each other.

RESULTS

### Phylogenetic signal and performance of predictor models

Across the full dataset of 223 archosauromorphs, there is a strongly significant phylogenetic signal in the skull–femur ratio for all time-calibrated trees (all $\lambda > 0.84$;

$p < 0.0001$). Phylogenetic signal results for all 40 time-calibrated trees can be found in Table S3.

Comparisons between the AIC scores for all 15 predictor models fitted to archosauromorph skull–femur lengths generally show similar levels of support (Fig. 1; AIC scores for all 40 trees from all predictor models can be found in Table S4). All models except one exhibit mean average AIC scores between 1.2 and −40.98 and median scores between −24.18 and −69.96 (Fig. 1; Table S4). The exception is the biotope model which shows the weakest level of support (i.e. higher AIC values; mean 77.7, median 53.1; Fig. 1). The 'taxonomy + diet + locomotory mode' model shows marginally the strongest level of support (mean −40.98, median −69.67; Fig. 1; Table S4). Method of time-calibration appears to have little effect on AIC scores for each model. Hereafter, only results from one randomly chosen tree from each time-scaling approach from the no predictor model are presented.

PGLS scaling relationships

For all studied archosauromorphs, skull length statistically significantly correlates with femur length for both time-scaled trees ($p < 0.0001$; Fig. 2). When slopes are considered, skull length scales with negative allometry with respect to femur length ($a = 0.81 \pm 0.077$ and 0.809 ± 0.088 for the *mbl*.1 and *cal3* trees, respectively; Fig. 2; Table 1). Archosauromorph skulls therefore become disproportionately smaller with increasing body size (see Table S5 for full PGLS results). When archosauromorphs are categorized into subsets according to taxonomic group, we find that skull length is strongly correlated with femur lengths in all groups except in basal Ornithischia ($p = 0.461$ and 0.421 for the *mbl*.1 and *cal3* ornithischian trees, respectively; Table 1), probably due to its small sample size ($n = 6$). When slopes are considered, skull length scales with positive allometry in basal archosauromorphs for both time-scaling methods (Table 1). Skull length scales with negative allometry for both time-scaling methods in ceratopsians, dinosaurs and sauropodomorphs (Table 1). Avialan skull length scales with negative allometry in the *cal3* tree, but scales with isometry in the *mbl*.1 tree (Table 1). Skull length scales isometrically with femur length in both time-calibrated trees in crocodylomorphs, ornithopods, pterosaurs, theropods and thyreophorans (Table 1; see Fig. S1 for regression lines and 95% confidence intervals for each taxonomic group; also see Fig. S2 for regression lines and 95% confidence intervals for all predictor subsets that show different scaling relationships between the *mbl*.1 and *cal3* trees). In the Archosauromorpha and Dinosauria with excluded sauropodomorphs subsets, skull lengths scale with negative
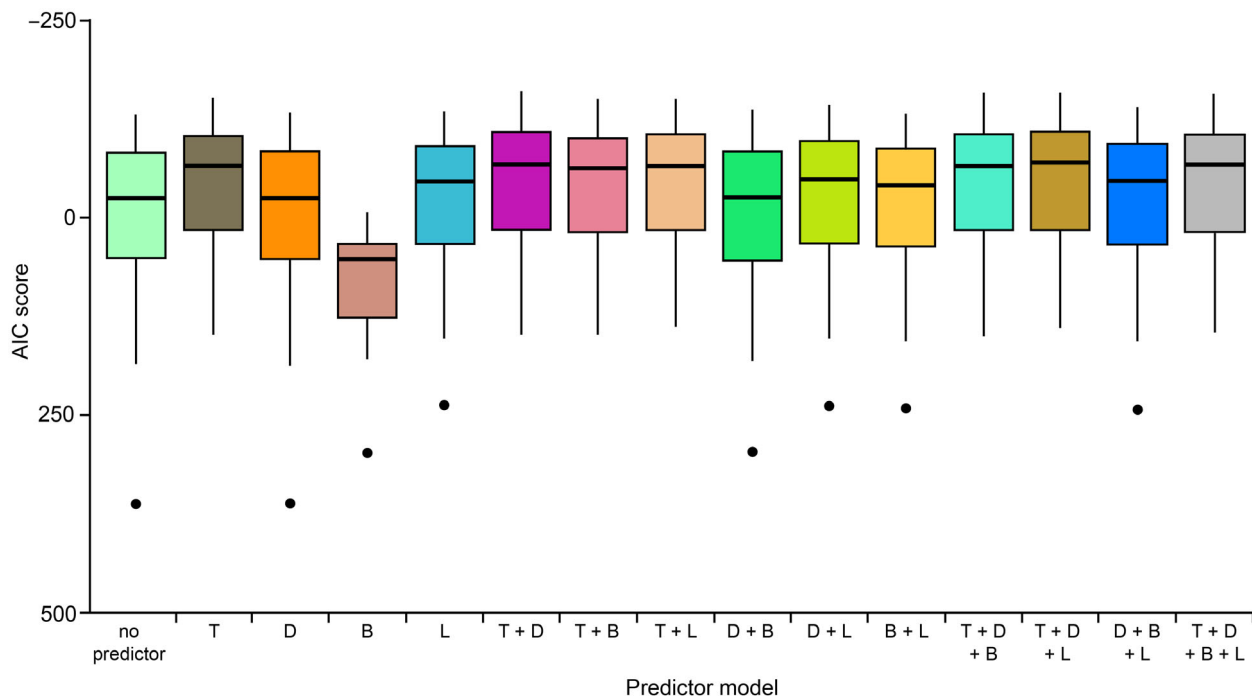
FIG. 1. Boxplots showing AIC scores of the predictor models fitted to archosauromorph phylogeny and log skull-length/log femur-length data using 40 randomly resolved, time-calibrated trees, 20 calibrated with the *mbl*.1 method and 20 with the *cal3* method. *Abbreviations*: T, taxonomy; D, diet; B, biotope; L, locomotory mode. Additive effects between predictors were modelled in all multi-predictor models (see text for further information). Box plot colours are for aesthetic purposes only. AIC scores of all models from each time-calibrated tree can be found in Table S4.

allometry in both time-calibrated trees (Table 1; Fig. S3; Table S5).

When categorized by diet, skull length is strongly correlated with femur length in both archosauromorph carnivores and herbivores for both time-calibrated trees (Fig. 3; Table 2). Carnivore skull lengths scale isometrically with respect to femur length for both time-scaled trees, while herbivore skull lengths scale with negative allometry (Fig. 3; Table 2). When categorized by locomotory mode, skull length is strongly correlated with femur length for all locomotory modes for both time-scaling methods (Table 3; see Fig. S4 for regression lines and 95% confidence intervals for each locomotory mode). Skull length scales with negative allometry for both time-calibrated trees in bipedal archosauromorphs and scales isometrically in biped-flying and quadrupedal archosauromorphs (Table 3). In facultatively quadrupedal archosaurs, skull length scales with negative allometry using the *mbl*.1 tree but scales isometrically using the *cal3* tree (Table 3). When assigned by biotope, skull length is strongly correlated with femur length for all three biotopes from both time-calibrated trees (Table 4; see Fig. S5 for regression lines and 95% confidence intervals for each biotope). From both time-calibrated trees, skull length scales isometrically in aerial archosauromorphs, with positive allometry in aquatic

archosauromorphs, and with negative allometry in terrestrial archosauromorphs (Table 4; Fig. S4). Both terrestrial basal archosauromorph carnivores and terrestrial dinosaur carnivores exhibit statistically significant relationships between skull and femur lengths (Fig. 4; Table 5). Skull length scales isometrically with femur length from both time-calibrated trees in dinosaurs, while in basal archosauromorphs, skull length scales isometrically with femur length from the *mbl*.1 tree, but scales with positive allometry from the *cal3* tree (Fig. 4; Table 5).

Ancestral skull–femur ratio estimates

The skull–femur ratio ancestral state estimates using the two time-calibrated trees show broadly similar estimated ratios across most archosauromorph lineages and for specific nodes of interest (Fig. 5; Table 6; see Table S6 for ancestral estimates, variance, and upper and lower 95% intervals for all nodes highlighted in Fig. 5, and for the complete ancestral estimate list of all 222 nodes from the two time-calibrated trees; see Fig. S6 for the locations of all 222 nodes within the two trees). The ancestral estimate of Archosauromorpha (node 1, Fig. 5) from the *mbl*.1 tree indicates a skull equal in length to that of the femur
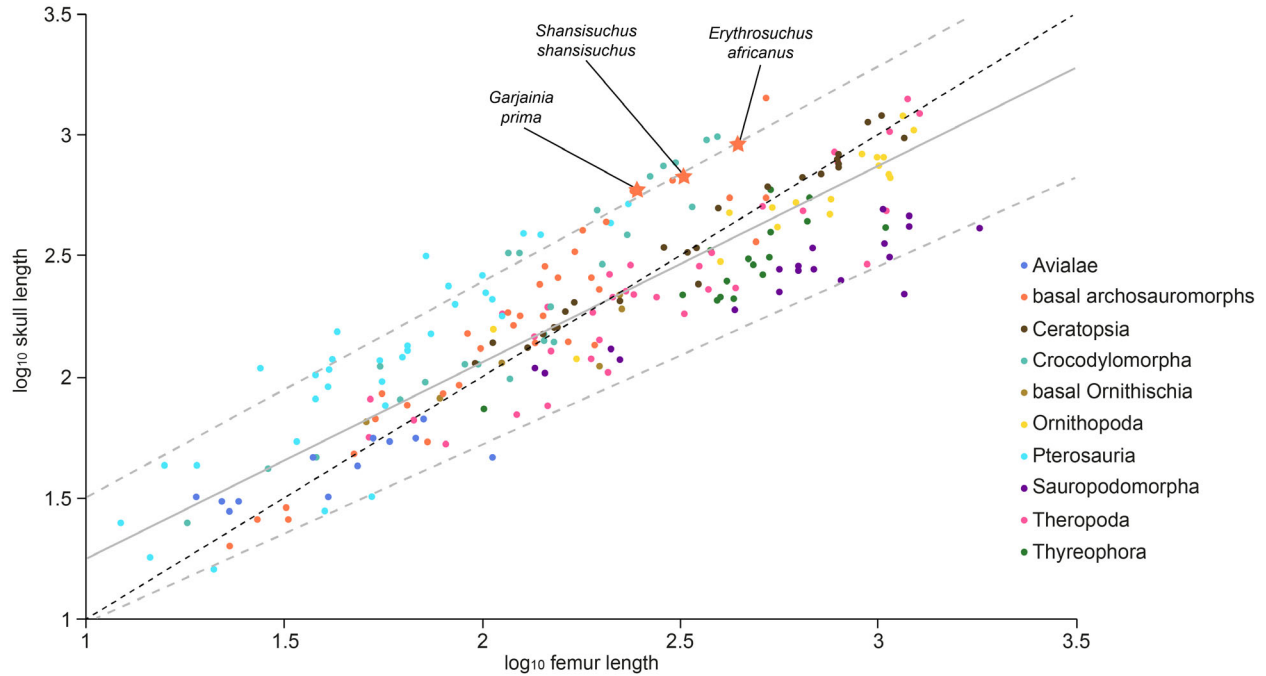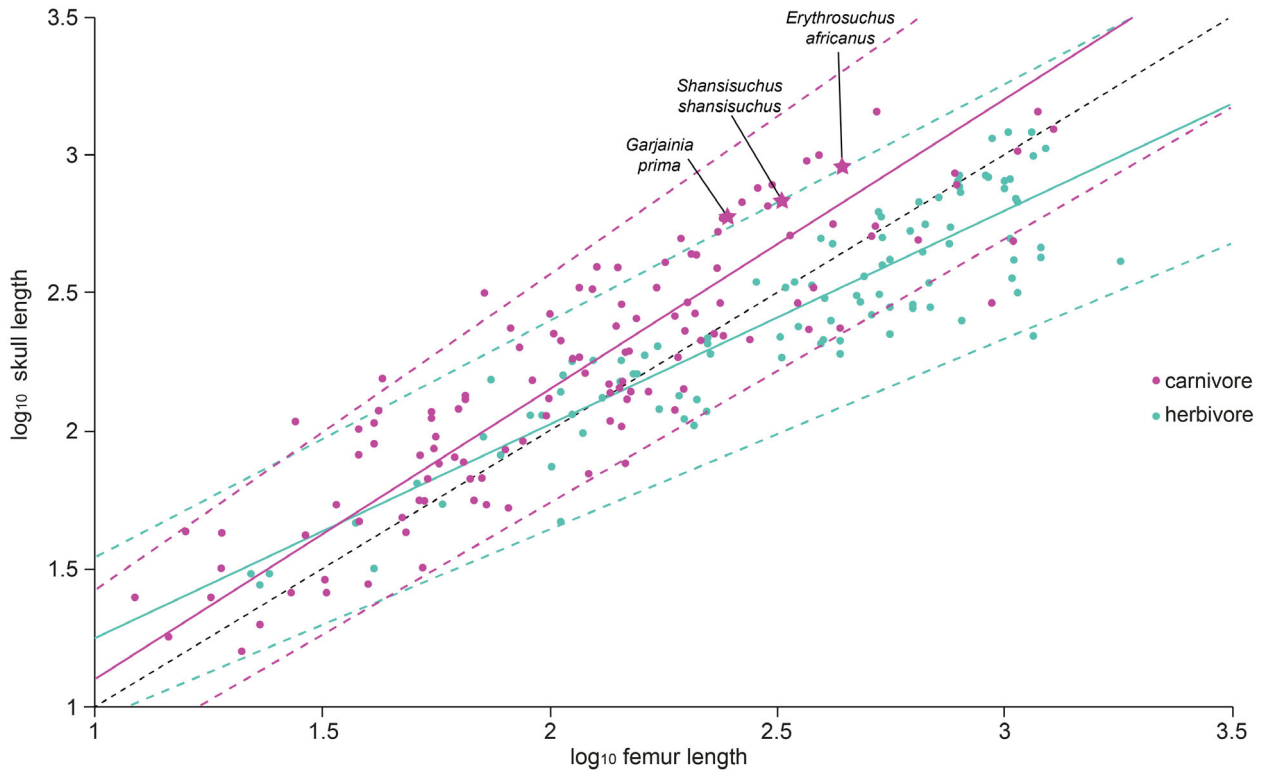
FIG. 2. Phylogenetic generalized least squares (PGLS) regression of log skull-length and log femur-length for 223 extinct archosauromorph species (grey solid line). Taxonomic clades and grades that comprise the dataset are highlighted. Star symbols denote erythrosuchids. Dashed grey lines denote 95% confidence intervals (CIs). Regression line and CIs from the analysis that used the *mbl*.1 time-scaled phylogeny. Taxa located above the regression line have disproportionately larger skulls and taxa located below the regression line have disproportionately smaller skulls. The theoretical isometric line ($a = 1$) is denoted by the dashed black line. PGLS results of all archosauromorphs from all 40 time-calibrated trees, as well as regression results of each taxonomic clade and grade from the *mbl*.1 and *cal3* tree, can be found in Table S5.

TABLE 1. Phylogenetic generalized least squares (PGLS) regression results of log skull-length and log femur-length for all studied archosauromorphs and for assigned taxonomic groups within Archosauromorpha.

Taxonomic group	df	*mbl*.1			*cal3*		
		Slope	95% CI	p	Slope	95% CI	p
All archosauromorphs	222	0.81	0.077	<0.0001	0.809	0.088	<0.0001
Avialae	11	0.735	0.284	0.0002	0.622	0.267	0.0004
Basal archosauromorphs	36	1.193	0.147	<0.0001	1.209	0.145	<0.0001
Ceratopsia	24	0.85	0.147	<0.0001	0.801	0.107	<0.0001
Crocodylomorpha	23	1.075	0.153	<0.0001	1.112	0.16	<0.0001
Dinosauria	116	0.761	0.114	<0.0001	0.679	0.1	<0.0001
Basal Ornithischia	5	0.424	1.445	0.461	0.401	1.245	0.421
Ornithopoda	16	0.894	0.242	<0.0001	0.92	0.267	<0.0001
Pterosauria	32	0.993	0.184	<0.0001	0.926	0.273	<0.0001
Sauropodomorpha	18	0.753	0.23	<0.0001	0.774	0.191	<0.0001
Theropoda	33	0.758	0.311	<0.0001	0.81	0.294	<0.0001
Thyreophora	15	1.242	0.414	<0.0001	1.32	0.519	<0.0001
Archosauromorpha without Sauropodomorpha	203	0.791	0.127	<0.0001	0.771	0.087	<0.0001
Dinosauria without Sauropodomorpha	97	0.817	0.129	<0.0001	0.837	0.138	<0.0001

Includes regression results using the *mbl*.1 and *cal3* time-calibrated trees and 95% confidence interval (CI) range for each tree. See text for how each taxonomic group was defined in this study. Full results for each PGLS can be found in Table S5.

FIG. 3. Phylogenetic generalized least squares (PGLS) regression results of log skull-length and log femur-length for 233 extinct archosauromorph species assigned as either carnivores (violet solid line) or herbivores (turquoise solid line). Star symbols denote erythrosuchids. Dashed lines indicate 95% confidence intervals (CIs) for the corresponding diet. Regression lines and CIs from the analysis that used the *mbl*.1 time-scaled phylogeny. Taxa located above the regression lines have disproportionately larger skulls and taxa located below the regression lines have disproportionately smaller skulls. The theoretical isometric line ($a = 1$) is denoted by the dashed black line.

TABLE 2. Phylogenetic generalized least squares (PGLS) regression results of log skull-length and log femur-length for all studied archosauromorphs assigned to a dietary group.

Diet	df	*mbl*.1			*cal3*		
		Slope	95% CI	p	Slope	95% CI	p
Carnivores	123	1.05	0.094	<0.0001	1.082	0.1	<0.0001
Herbivores	98	0.777	0.083	<0.0001	0.718	0.08	<0.0001

Includes regression results using the *mbl*.1 and *cal3* time-calibrated trees and 95% confidence interval (CI) range for each tree. See text for how each dietary group was defined in this study. Full results for each PGLS can be found in Table S5.

(1.033 ± 0.059), whereas the estimate from the *cal3* tree indicates a slightly longer skull (1.056 ± 0.05; Table 6). The ancestral *mbl*.1 and *cal3* estimates for Erythrosuchidae (node 2) in contrast clearly show a disproportionately larger skull (Fig. 5; Table 6). The ancestral estimates for the most recent common ancestor of Archosauria (node 3) denotes a skull only very slightly longer than the femur, but while the same trend is observed in the most recent common ancestor of Pseudosuchia (node 17), the ancestral estimate for the most recent common ancestor of Avemetatarsalia (node 4) shows a skull and femur of equal length (Table 6). Ancestral estimates for the two major avemetatarsalian clades, Pterosauria and Dinosauria (nodes 5 and 6 respectively), show a strongly disproportionately large skull for the former and a skull and femur of equal length in the latter (Table 6). The ancestral estimate for Ornithischia (node 7, Fig. 5) from the *mbl*.1 tree indicates a disproportionately short skull (albeit marginally), while the *cal3* tree indicates a skull equal in length to the femur.

TABLE 3. Phylogenetic generalized least squares (PGLS) regression results of log skull-length and log femur-length for all studied archosauromorphs assigned to a locomotory mode.

Locomotory mode	df	*mbl*.1			*cal3*		
		Slope	95% CI	p	Slope	95% CI	p
Bipedal	56	0.786	0.199	<0.0001	0.781	0.176	<0.0001
Bipedal-quadrupedal	21	0.725	0.273	<0.0001	0.862	0.182	<0.0001
Bipedal-flying	45	0.832	0.182	<0.0001	0.832	0.294	<0.0001
Quadrupedal	97	1	0.096	<0.0001	1.059	0.105	<0.0001

Includes regression results using the *mbl*.1 and *cal3* time-calibrated trees and 95% confidence interval (CI) range for each tree. See text for how each locomotory mode was defined in this study. Full results for each PGLS can be found in Table S5.

TABLE 4. Phylogenetic generalized least squares (PGLS) regression results of log skull-length and log femur-length for all studied archosauromorphs assigned to an inhabited biotope.

Biotope	df	*mbl*.1			*cal3*		
		Slope	95% CI	p	Slope	95% CI	p
Aerial	45	0.832	0.182	<0.0001	0.84	0.289	<0.0001
Aquatic	26	1.213	0.15	<0.0001	1.222	0.129	<0.0001
Terrestrial	149	0.87	0.097	<0.0001	0.853	0.094	<0.0001

Includes regression results using the *mbl*.1 and *cal3* time-calibrated trees and 95% confidence interval (CI) range for each tree. See text for how each biotope was defined in this study. Full results for each PGLS can be found in Table S5.
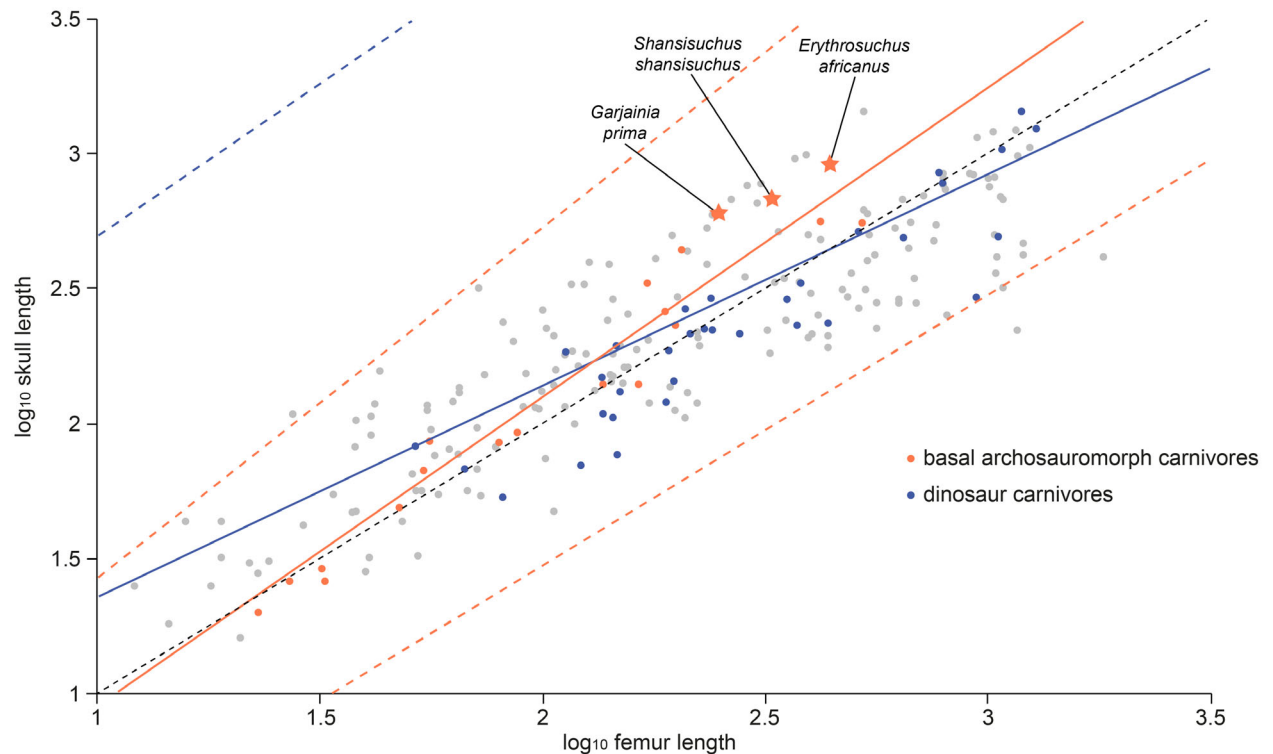
FIG. 4. PGLS results of log skull-length and log femur-length for terrestrial basal archosauromorph carnivores (orange solid line) and terrestrial dinosaur carnivores (blue solid line). Star symbols denote erythrosuchids. Dashed lines indicate 95% confidence intervals (CIs) for the corresponding category. Regression lines and CIs from the analysis that used the *mbl*.1 time-scaled phylogeny. Taxa located above the regression lines have disproportionately larger skulls and taxa located below the regression lines have disproportionately smaller skulls. Non-applicable archosauromorphs are greyed out for easier comparison. The theoretical isometric line (*a* = 1) is denoted by the dashed black line.

TABLE 5. Phylogenetic generalized least squares (PGLS) regression results of log skull-length and log femur-length for terrestrial basal archosauromorph carnivores and terrestrial dinosaur carnivores.

Category	df	*mbl*.1			*cal3*		
		Slope	95% CI	p	Slope	95% CI	p
Basal archosauromorphs	19	1.149	0.154	<0.0001	1.244	0.178	<0.0001
Dinosaurs	32	0.784	0.341	<0.0001	0.804	0.369	<0.0001

Includes regression results using the *mbl*.1 and *cal3* time-calibrated trees. Includes 95% confidence interval (CI) range. Full results for each PGLS can be found in Table S5.

Ancestral estimates for several major dinosaurian clades, including the most recent common ancestors of Ceratopsia, Ornithopoda, Sauropodomorpha and Theropoda (nodes 9–12 respectively), indicate skulls and femora of equal length (Fig. 5; Table 6), which then exhibit steady directional changes in skull–femur ratio through evolutionary time. For example, the sauropodomorph ratio becomes smaller through time, while the ceratopsian ratio becomes slightly larger (Fig. 5). Multiple independent shifts towards disproportionately shorter or longer skulls are optimized in Theropoda and in Avialae (nodes 12 and 16 respectively; Fig. 5). For example, the ancestral estimates for Abelisauroidea (node 13; Fig. 5; Table 6) indicate skulls and femora of equal length with multiple lineages independently evolving disproportionately smaller skulls. In contrast, ancestral estimates of Carnosauria and Tyrannosauroidea (nodes 14 and 15 respectively) indicate skulls and femora of equal length (Table 6) with little change exhibited by subsequent lineages and taxa (Fig. 5). The ancestral ratio estimate for Thyreophora (node 8) indicates a disproportionately short skull (Table 6), and the ratio in this clade exhibits little change through evolutionary time (Fig. 5). Interestingly, the ancestral estimates for Loricata and Crocodylomorpha (nodes 18 and 19 respectively) indicate skulls and femora of equal length (Table 6), with multiple lineages within the latter clade subsequently evolving disproportionately longer skulls (Fig. 5).

DISCUSSION

Scaling relationships and drivers of relative skull size

Our results indicate that skull–femur ratios across Archosauromorpha are largely determined by phylogeny and indicate no clear support for any of our predictor models as an explanation behind the observed patterns. However, the biotope model provides a relatively poorer explanation for skull–femur ratios than other models. Multiple, unrelated selection pressures could explain the weak support for our predictor models, since multiple pressures acting on anatomical structures that perform multiple roles can result in morphologies that are not optimally adapted for a single role (Gould & Lewontin 1979; Fisher 1985; Ferry-Graham *et al.* 2002). Nevertheless, our results can still be discussed in ecological and evolutionary contexts.

Our scaling relationships are only slightly influenced by time-scaling method, thus our results from the two time-scaled trees can be discussed together. Relative skull size scaling with negative allometry for all studied archosauromorphs considered together contrasts with similar studies of extant mammalian clades. For example, skull sizes of multiple groups of marsupials (Macropodidae) and placentals (Chiroptera, Primates, Rodentia, Ungulata) scale isometrically with respect to body size (Cardini & Polly 2013; Cardini *et al.* 2015; Cardini 2019), while skull sizes

FIG. 5. Ancestral character-state reconstruction of log skull-length/log femur-length ratio evolution for 223 archosauromorphs from mapping ratios onto time-calibrated supertrees. A, reconstruction using the *mbl*.1 dating method. B, reconstruction using the *cal3* dating method. Tree number [1] from the 20 randomly resolved pruned supertrees from each dating method are shown here. Highlighted nodes: 1, Archosauromorpha; 2, Erythrosuchidae; 3, Archosauria; 4, Avemetatarsalia; 5, Pterosauria; 6, Dinosauria; 7, Ornithischia; 8, Thyreophora; 9, Ceratopsia; 10, Ornithopoda; 11, Sauropodomorpha; 12, Theropoda; 13, Abelisauroidea; 14, Carnosauria; 15, Tyrannosauroidea; 16, Avialae; 17, Pseudosuchia; 18, Loricata; 19, Crocodylomorpha. Reconstructed values of the highlighted nodes, along with the variance and upper and lower 95% confidences intervals, can be found in Table S6. Silhouettes not to scale and adapted from http://www.phylopic.org/ under a Creative Commons Attribution NonCommerical ShareAlike 3.0 Unported license (https://creativecommons.org/licenses/by-nc-sa/3.0/) except where stated. Anticlockwise from 'non-archosaurian archosauromorphs': *Erythrosuchus africanus*, Emilio Lopez-Rolandi; *Preondactylus buffarinii*, Mark Witton; *Heterodontosaurus tucki*, Scott Hartman; *Stegosaurus stenops*, Andrew Farke; *Triceratops porosus*, no copyright; *Iguanodon bernissartensis*, Jamie Headden; *Barosaurus lentus*, Scott Hartman; *Tyrannosaurus rex*, Scott Hartman; *Archaeopteryx lithographica*, no copyright; *Postosuchus kirkpatricki*, no copyright; *Torvoneustes carpenter*, Dmitry Bogdanov and T. Michael Keesey.
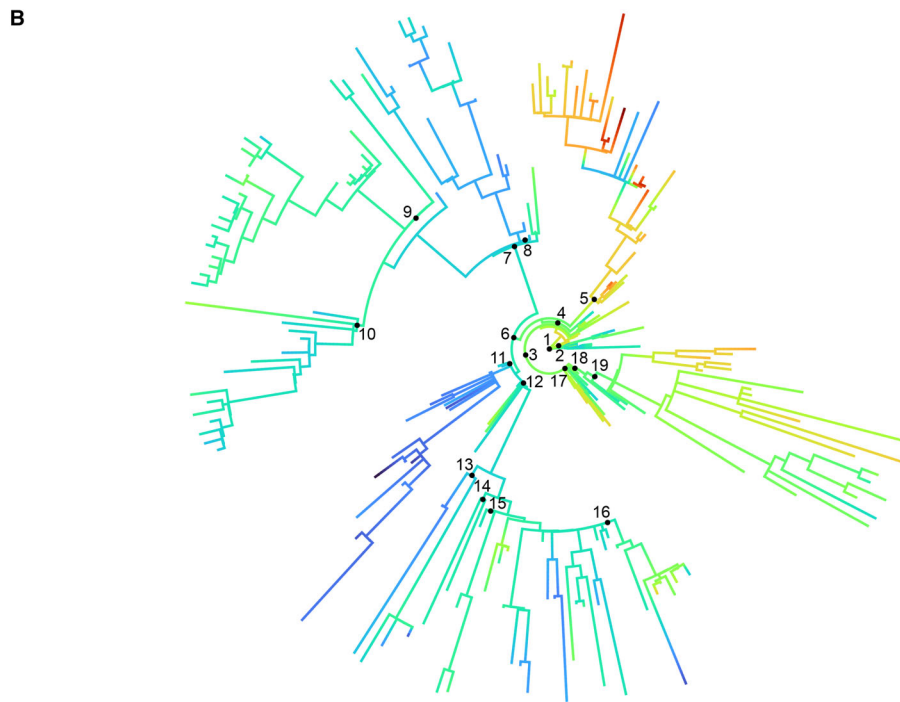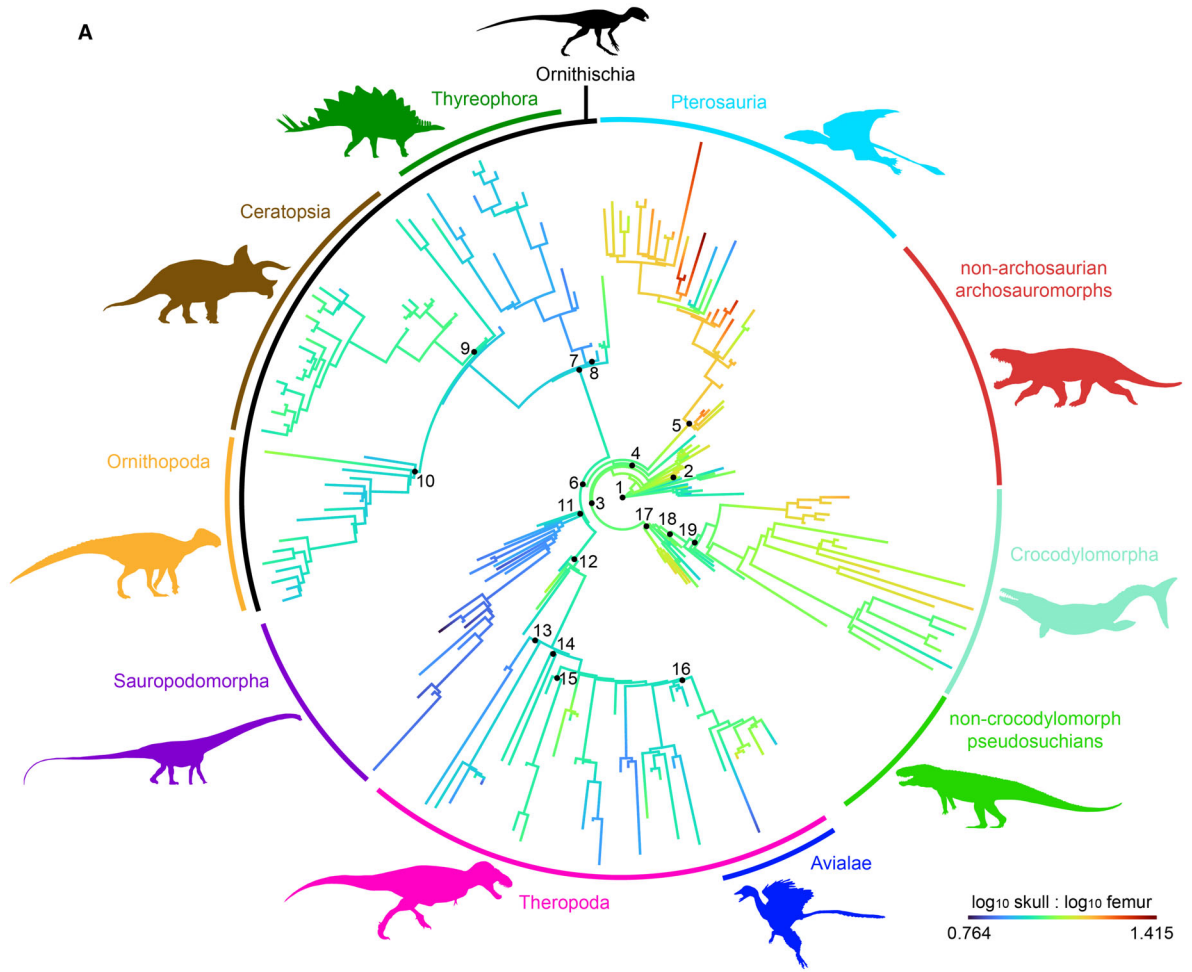
TABLE 6. Estimated ancestral archosauromorph log skull-length/log femur-length ratios, and 95% confidence interval (CI) range, for selected nodes from the *mbl*.1 and *cal3* time-calibrated trees.

Node no.	Node label	*mbl*.1 ancestral ratio estimate	±95% CI	*cal3* ancestral ratio estimate	±95% CI
1	Archosauromorpha	1.033	0.059	1.056	0.050
2	Erythrosuchidae	1.146	0.027	1.163	0.002
3	Archosauria	1.043	0.040	1.064	0.032
4	Avemetatarsalia	1.036	0.042	1.049	0.049
5	Pterosauria	1.174	0.051	1.154	0.083
6	Dinosauria	1.000	0.046	0.994	0.060
7	Ornithischia	0.953	0.043	0.961	0.052
8	Thyreophora	0.941	0.038	0.943	0.042
9	Ceratopsia	0.994	0.210	1.006	0.012
10	Ornithopoda	0.963	0.043	0.992	0.063
11	Sauropodomorpha	0.984	0.046	0.964	0.410
12	Theropoda	0.998	0.052	0.970	0.042
13	Abelisauroidea	0.960	0.060	0.943	0.122
14	Carnosauria	0.969	0.063	0.982	0.115
15	Tyrannosauroidea	0.982	0.053	0.991	0.072
16	Avialae	0.974	0.037	0.985	0.046
17	Pseudosuchia	1.046	0.042	1.064	0.032
18	Loricata	1.038	0.050	1.050	0.050
19	Crocodylomorpha	1.024	0.049	1.031	0.087

Node numbers correspond to those indicated in Figure 5. Full ancestral estimate reconstructions can be found in Table S6. All values to 3 d.p.

of other placentals (Carnivora, Cetacea) scale with positive allometry (Slater & Van Valkenburgh 2009; Tamagnini *et al.* 2017; Law *et al.* 2018). Skull sizes also scale with positive allometry in a few unrelated extant avian lineages, although these relationships are less clear (Bright *et al.* 2016; Linde-Medina 2016; Tokita *et al.* 2016). Our results therefore indicate that relative skull size relationships may not be universal between major groups of distantly related amniotes and that focusing on scaling relationships of data subsets may enable identification of more informative patterns.

With regard to taxonomic subsets, it is unsurprising that basal archosauromorph skulls scale with positive allometry, given that several distinct groups, including erythosuchids, proterochampsids, proterosuchids and phytosaurs are frequently cited as having disproportionately large skulls (e.g. Stocker & Butler 2013; Butler *et al.* 2019; Ezcurra *et al.* 2020*b*). There is also emerging evidence of disproportionately large skulls in basal aetosaurs (e.g. *Revueltosaurus callenderi*; Parker *et al.* 2021). However, this study provides some of the first quantitative evidence that the skulls of these lineages are indeed disproportionately larger for their size in comparison to other archosauromorphs (Butler *et al.* 2019). Since all our studied basal archosauromorphs are from the Triassic, this allometric relationship highlights the uniqueness of not only Triassic archosauromorphs but Triassic ecosystems in general.

A more surprising result perhaps, given the huge morphological disparity exhibited by the clade, is the number of archosaurian groups that exhibit isometric scaling of skull length with respect to femur length. For example, the relationship in non-avialan theropods contrasts with that found by Therrien & Henderson (2007), in which skull lengths scaled with positive allometry with respect to body length. However, that study used a considerably smaller sample size in terms of both number of species and number of represented theropod subclades. Due to the nature of the fossil record, over half of our theropod sample were coelurosaurs; those species more closely related to *Passer domesticus* than to *Allosaurus fragilis* (*sensu* Turner *et al.* 2012). Coelurosaurian theropods exhibit rapid and sustained morphological changes moving crownward towards Avialae, such as miniaturization (the main exceptions being tyrannosauroids and ornithomimosaurs), truncation of the snout and modifications of the limb bones, which are all likely to have influenced relative skull size (Bhullar *et al.* 2012; Benson & Choiniere 2013; Dececchi & Larsson 2013; Brusatte *et al.* 2014; Lee *et al.* 2014*b*, 2020; Puttick *et al.* 2014; Foth *et al.* 2016*b*; Nebreda *et al.* 2021). This larger coverage of taxa potentially explains the difference between our results and those of Therrien & Henderson (2007), and highlights the importance of thorough species sampling.

Another surprising result is the isometric scaling found for Crocodylomorpha. The Mesozoic witnessed the highest morphological and ecological diversity of crocodylomorphs, particularly in the Jurassic and Cretaceous, including: small cursorial forms; specialized herbivores; semi-aquatic and fully marine piscivores and carnivores; and terrestrial apex predators (Young *et al.* 2010; Stubbs *et al.* 2013; Ősi 2014; Melstrom & Irmis 2019; Wilberg *et al.* 2019; Montefeltro *et al.* 2020). A range of skull morphologies is thereby exhibited by Mesozoic crocodylomorphs, from the short stubby rostra of notosuchians such as *Simosuchus clarki* to the gracile elongate rostra of thalattosuchians such as *Cricosaurus suevicus* (Felice *et al.* 2021; Stubbs *et al.* 2021). It is therefore possible that these morphological extremes effectively balance the overall trend and that greater focus on specific crocodylomorph lineages may reveal further interesting patterns.

Focusing on specific ornithischian lineages reveals interesting patterns, namely negative allometric scaling in ceratopsians, while ornithopods and thyreophorans scale isometrically. Our ceratopsian relationship contrasts with previous research that found ceratopsian skulls to scale isometrically (VanBuren *et al.* 2015). As both studies have very similar ceratopsian samples, these differences could be due to the choice of time-scaling methods. For example, both studies used the *mbl* method and our *mbl*.1 tree produced a slope with confidence intervals only just outside the theoretical slope of isometry. Our *cal3* tree, a method not used by VanBuren *et al.* (2015), in contrast produced a slope with a much lower gradient. Nevertheless, these results are still worth mentioning within evolutionary and ecological contexts. It is likely that the negative scaling relationship is being driven by the appearance of disproportionately large skulls very early in ceratopsian evolutionary history, such as *Psittacosaurus major* and *Psittacosaurus sinensis*, although the exact reasons behind this are unclear (Ostrom 1966; Sereno *et al.* 2007; VanBuren *et al.* 2015).

With regard to the dietary subsets, carnivores exhibiting proportionally larger skulls than herbivores is unsurprising as larger skulls have more jaw muscle attachment sites for higher bite forces, are capable of wider gapes, and have greater resistance to biomechanical stress and strain, all of which aid in the capture and killing of prey (Slater & Van Valkenburgh 2009; Fabre *et al.* 2016; McCurry *et al.* 2017; Galatius *et al.* 2020). In contrast, consumption of fibrous and tough plant material often correlates with modified postcranial structures that enable effective digestion including, but not exclusive to, elongate intestinal tracts, gastric mills and increased trunk size (Barrett 2014; and references therein). However, the isometric scaling of carnivore skull size contrasts with several groups of mammalian carnivores that exhibit positive allometric scaling of skull size with respect to both body

size and the size of preferred prey (e.g. carnivorans and cetaceans; Slater & Van Valkenburgh 2009; Tamagnini *et al.* 2017; Galatius *et al.* 2020; but see Law *et al.* 2018). Isometric scaling could be explained by the scaling relationships of our terrestrial carnivore subsets. The isometric dinosaur carnivore scaling relationship may have been influenced by the relative lack of spinosaurids and carcharodontosaurids (lineages that are regarded as hypercarnivorous and which show evidence of proportionately large skulls; Sereno *et al.* 1998; Sues *et al.* 2002; Novas *et al.* 2013) due to incomplete preservation. Carnivores that probably filled mesopredator niches (such as dromaeosaurids and troodontids; Wick *et al.* 2015) would have experienced lower selection pressure for larger skulls, occurred in greater numbers, and may therefore have lowered the slope gradient (Tamagnini *et al.* 2017; Galatius *et al.* 2020). Nevertheless, we include taxa from these hypothesized hypercarnivorous lineages where preservation allowed, as well as other lineages of large theropods such as tyrannosaurs and ceratosaurs (Benson *et al.* 2018). In addition, recent evidence that suggests a semi-aquatic lifestyle for some spinosaurids (Ibrahim *et al.* 2020), potentially excluding them from this terrestrial subset. We therefore regard our terrestrial dinosaur carnivore sampling range and the resulting slope to be representative despite the limitations of the fossil record.

Locomotory mode may also help to explain scaling similarities and differences between archosauromorph carnivores and mammalian carnivores. For example, the vast majority of theropods are bipedal and therefore have a centre of mass located around the hips allowing the animal to maintain balance (Henderson 1999; Maidment *et al.* 2014). Theoretical modelling has shown that even small morphological changes to the skulls and/or forelimbs of bipedal dinosaurs can move the centre of mass anteriorly, resulting in a top-heavy animal (Maidment *et al.* 2014; Barrett & Maidment 2017). Bipedality therefore probably imposes stronger constraints on skull size than quadrupedality. This is further exemplified by the quadrupedal erythrosuchids (*Erythrosuchus africanus*, *Garjainia prima* and *Shansisuchus shansisuchus*), which not only have the most disproportionately large skulls among terrestrial archosauromorph carnivores, but also among all terrestrial taxa in this study. In contrast, the two non-crocodylomorph loricatans *Postosuchus* and *Prestosuchus* have relative skull sizes more similar to those of hypercarnivorous theropods than to erythrosuchids. In fact, hypothesized Triassic mesopredators such as ornithosuchids (von Baczko 2018) exhibit proportionately longer skulls than the aforementioned loricatans (although loricatan skulls are alternatively much deeper; Chatterjee 1985; Weinbaum 2011; Mastrantonio *et al.* 2019). These scaling relationships between basal archosauromorphs and dinosaurs, and their skull–femur length ratios, indicate

that disproportionately large skulls are not a prerequisite for hypercarnivory and further highlights the morphological uniqueness of erythrosuchids.

With regard to the biotope subsets, different scaling relationships between our subsets are broadly similar to morphological studies of extant and extinct squamate skulls that found that mode of life (terrestrial, fossorial, semi-aquatic etc.) was a strong driver of skull shape and size (Fabre *et al.* 2016; da Silva *et al.* 2018). It is likely that the negative allometry seen in the scaling of terrestrial archosauromorph skulls is driven by the disproportionately small skulls of sauropodomorphs and thyreophorans (Christiansen 1999). Isometric scaling of aerial archosauromorph skulls is consistent with a similar pattern observed in extant bats (Chiroptera; Cardini & Polly 2013). Powered flight has independently evolved in archosauromorphs at least twice (at the base of Pterosauria and near the base of Avialae), and possibly even three or more times (at least once within Deinonychosauria, such as in *Microraptor zhaoianus*; Pei *et al.* 2020), with each clade exhibiting marked modifications and reductions of skeletal elements for balance and flight efficiency (Bell *et al.* 2011; Benson *et al.* 2014, 2018; Lee *et al.* 2014b; Tokita 2015; Witton 2015). For example, the hind limbs of pterosaurs and bats are directly connected to the forelimbs via the brachypatagium and are thus part of the flight apparatus, while avialan hind limbs are not involved in flight and can move independently of the forelimbs (Tokita 2015). It is therefore interesting that morphological adaptations for flight do not change skull scaling relationships from the ancestral state, not just in archosauromorphs, but in all aerial amniotes.

Disproportionately large skulls and positive allometric scaling in unrelated aquatic archosauromorphs can be explained by ecomorphological convergence. Extant crocodilians are all semi-aquatic and also exhibit disproportionately large skulls (VanBuren *et al.* 2015; Butler *et al.* 2019). This seems to be the result of some degree of cranial elongation driven by heterochronic modifications in craniofacial ontogeny that facilitated seizing prey via unilateral biting motions (Erickson *et al.* 2012; Walmsley *et al.* 2013; McCurry *et al.* 2015; Morris *et al.* 2019; Lee *et al.* 2020), and by reduced limb sizes since elongated neural spines of the caudal vertebrae enable swimming via axial muscle-derived propulsion (Pol *et al.* 2012; Grigg & Kirshner 2015; Molnar *et al.* 2015; Henderson 2018). Shifts from terrestrial to semi or fully aquatic lifestyles in extinct archosauromorphs have occurred at least once in each of the following clades: Tanystropheidae, Proterosuchidae; Proterochampsia; Phytosauria; and Crocodylomorpha (Ezcurra 2016; Wilberg *et al.* 2019; Brown *et al.* 2020; Ezcurra *et al.* 2020b). In most cases (not tanystropheids and at least some non-proterochampsid proterochampsians) these lineages exhibit some level of

convergence with crocodilians and with each other, resulting in disproportionately large skulls (Stocker & Butler 2013; Trotteyn *et al.* 2013; Wynd *et al.* 2019; Brown *et al.* 2020; Ezcurra *et al.* 2020b; Felice *et al.* 2021; Stubbs *et al.* 2021). Selection for larger skull–femur ratios would also be greater in semi-aquatic taxa as they are more likely to spend time in water, in which smaller limbs and larger axial muscles, to reduce drag and combat locomotion-induced stresses, respectively, would be more advantageous (Biewener 2005; Montgomery *et al.* 2013; Molnar *et al.* 2015).

Relative skull size evolution

The isometric, or near-isometric, ancestral skull–femur ratio estimates for the majority of our higher-level clades (i.e. above family level) indicates that minimal changes in relative skull size occur prior to the origin of a clade and that greater changes occur soon after the clade has appeared. This indicates that deviations of the ancestral skull–femur ratio probably happened once phylogenetic diversifications occurred, during a phase of ecomorphological expansion. For example, the isometric estimate for the ancestral sauropodomorph is quickly followed by a conspicuous ratio decrease in the lineage that includes all sauropodomorphs except for its two earliest-diverging members, *Buriolestes schultzi* and *Eoraptor lunensis*. This is consistent with developmental timing shifts and bauplan changes that began to occur around this time such as: the shortening and anterior rotation of cranial bones associated with the braincase (e.g. jugal); increasing trunk size; elongation of the neck and development of columnar limbs (Christiansen 1999; Sander *et al.* 2010; Rauhut *et al.* 2011; Sookias *et al.* 2012; Turner & Nesbitt 2013; Barrett & Maidment 2017; Fabbri *et al.* 2021; Pradelli *et al.* 2021). These changes are likely to have co-evolved with dietary shifts to bulk herbivory as sauropodomorphs became among the dominant herbivores of the latest Triassic and Early Jurassic (Christiansen 1999; Sander *et al.* 2010; Rauhut *et al.* 2011; Fabbri *et al.* 2021).

However, this is perhaps not the case for clades where multiple taxa and lineages exhibit independent changes in relative skull size. In pterosaurs for example, the abrupt decrease and almost immediate subsequent increase in relative skull size around the centre of the pterosaur tree is probably influenced by anurognathids; a family from the Middle–Upper Jurassic characterized by very small wingspans (<1 m) and short, box-like skulls (Bennett 2007; Bestwick *et al.* 2018). This morphology is hypothesized as an adaptation for a unique lifestyle among pterosaurs, that is, catching insects on the wing with their mouths open (Bestwick *et al.* 2018; and references therein). However, the influence of topological

uncertainties cannot be ruled out as other phylogenies recover anurognathids as one of the earliest branching groups (e.g. Lü *et al.* 2010; Rodrigues *et al.* 2015), which is likely to minimize these abrupt increase and decrease events due to a longer anurognathid ghost lineage. The repeated evolution of disproportionately large skulls in pterosaurs, particularly in derived lineages, could be due to multiple non-mutually exclusive selection pressures including less reliance on terrestrial locomotion as flight becomes more efficient, thereby reducing the size of the hind limbs (Witton & Habib 2010; Venditti *et al.* 2020), and the occupation of new niches as early-diverging lineages were small and most likely insectivorous while more deeply nested lineages became carnivores and piscivores (Bestwick *et al.* 2020). These patterns reflect the huge disparity in pterosaur relative skull sizes and may indicate fewer phylogenetic constraints from these flying reptiles relative to other archosauromorphs.

The multiple, independent skull–femur ratio decreases in theropods (including avialans) similarly indicate unappreciated patterns in body plan evolution. It is tempting to suggest that these decreases denote dietary shifts towards facultative or obligate herbivory such as in ornithomimosaurs and oviraptorosaurs (Barrett 2014). However, this is unlikely to be the sole explanation for two main reasons: (1) there is limited evidence that herbivory is a major driver in altering theropod skull and body sizes (Zanno & Makovicky 2013; Button & Zanno 2020); and (2) there are large theropods in our dataset (total body length >6 m) that show quantitative evidence of carnivory and have disproportionately short, yet deep, skulls, such as the abelisaurids *Carnotaurus sastrei* and *Skorpiovenator bustingorryi* (Bonaparte *et al.* 1990; Canale *et al.* 2009; Mazetta *et al.* 2009). Furthermore, our results show limited evidence of relative skull size increases in supposed hypercarnivorous lineages such as tyrannosauroids. These patterns suggest that hypercarnivory and herbivory are not necessary prerequisites for disproportionately large and small skulls, respectively, in theropods. Incorporating other skull size proxies in future investigations, such as skull depth, may help corroborate this emerging view.

Similar patterns in other non-theropod carnivores also cast doubt on the necessity for disproportionately large skulls. For example, the decrease in skull–femur ratio estimates between the slightly disproportionately large skull of the ancestral pseudosuchian and the subequal skull and femur lengths of the ancestral loricatan and crocodylomorph (Table S6) is contrary to what would be expected from a lineage containing a paraphyletic assemblage of hypothesized apex predators such as *Prestosuchus* and *Postosuchus* (Chatterjee 1985; Nesbitt 2011; Nesbitt *et al.* 2013; Desojo *et al.* 2020*a*). In contrast, the ancestral Erythrosuchidae ratio estimate (Table S6) indicates that disproportionately large skulls are probably a synapomorphic trait

for this clade (Ezcurra *et al.* 2013; Butler *et al.* 2019; Maidment *et al.* 2020). It can therefore be argued that the skull–femur ratios of carnivorous early loricatans are more like those of carnivorous theropods, such as tyrannosaurids, than those of erythrosuchids and that the erythrosuchid bauplan is morphologically unique among terrestrial archosauromorph carnivores with respect to their hugely disproportionately large skulls, short neck and quadrupedality. Further investigations into relative skull size convergence between distantly related archosauromorph carnivores, or even between archosauromorph and mammalian carnivores, could use non-uniform evolutionary models such as SURFACE as they do not require *a priori* assumptions on where regime shifts are located in the phylogeny (Ingram & Mahler 2013; Godoy *et al.* 2019).

It is worth noting that some of our skull–femur ratio estimates could be affected by limitations of the fossil record. For example, the high Pterosauria ancestral estimates are probably influenced by the absence of non-pterosaurian pterosauromorphs in our dataset due to their extremely rare and poorly preserved nature, with the earliest-known pterosaurs from the late Norian already exhibiting a highly modified bauplan capable of active flight (Dalla Vecchia 2013; Dean *et al.* 2016; Britt *et al.* 2018; Ezcurra *et al.* 2020*a*). The absence of earlier pterosauromorphs may thereby artificially affect the ancestral Pterosauria estimate. Similarly, the fossil record of early ornithischians from the Triassic and Early Jurassic is very poor or even null (Irmis *et al.* 2007; Baron 2017; but see Desojo *et al.* 2020*b*), which in our dataset creates a ghost lineage of approximately 35–40 myr from the base of Dinosauria to the earliest included ornithischian. This long ghost lineage is likely to have caused the ratio estimate differences between our two time-scaled trees. There is some published evidence that silesaurids, traditionally viewed as the sister group to Dinosauria, may actually be a paraphyletic assemblage of Triassic ornithischians that would greatly reduce the length of this ghost lineage (Cabreira *et al.* 2016; Müller & Garcia 2020). However, the lack of preservation of complete skulls also prevented their inclusion here. New, well-preserved fossil material and greater resolution of phylogenetic relationships will further improve the robustness of future studies.

CONCLUSION

Relative skull size in archosauromorphs is strongly phylogenetically structured, with diet, locomotory mode and biotope found as much weaker drivers of the observed scaling trends. Most significant changes in relative skull size occur soon after the origin of most terrestrial archosauromorph clades, which is indicative of an ecomorphological expansion (or evolutionary radiation) followed by relative

stasis. In addition, this study provides some of the first quantitative evidence that the skulls of erythrosuchid archosauriforms are disproportionately large for their body size and that this trend is distinct from the proportionately sized skulls of theropod dinosaurs and non-crocodylomorph loricatans. Furthermore, the disproportionately large skulls of erythrosuchids were unique not just among terrestrial carnivores, but among all terrestrial archosauromorphs. Our study therefore indicates that disproportionately large skulls are not a prerequisite for hypercarnivory in archosauromorphs and that Early and early Middle Triassic ecosystems were even more ecomorphologically diverse than previously thought.

Author contributions. **Conceptualization** R.J. Butler, S.C.R. Maidment, M.D. Ezcurra; **Data Curation** J. Bestwick, P.L. Godoy, R.J. Butler; **Formal Analysis** J. Bestwick, P.L. Godoy; **Funding Acquisition** R.J. Butler, J. Bestwick; **Investigation** M. Wroe, J. Bestwick, P.L. Godoy, T.J. Raven, J.A. Bonsor; **Methodology** J. Bestwick, R.J. Butler, P.L. Godoy, M.D. Ezcurra, S.C.R. Maidment; **Project Administration** J. Bestwick, R.J. Butler, M. Wroe; **Resources/Software** R.J. Butler, P.L. Godoy, J. Bestwick; **Supervision** R.J. Butler, S.C.R. Maidment; **Validation** J. Bestwick, P.L. Godoy; **Visualization** J. Bestwick, P.L. Godoy; **Writing – Original Draft** J. Bestwick; **Writing – Review & Editing** J. Bestwick, R.J. Butler, P.L. Godoy, M.D. Ezcurra, S.C.R. Maidment, J.A. Bonsor, T.J. Raven, M. Wroe.

Editor. Kenneth Angielczyk

SUPPORTING INFORMATION

Additional Supporting Information can be found online (https://doi.org/10.1111/pala.12599):

Fig. S1. PGLS results of log skull-length and log femur-length for each extinct archosauromorph taxonomic group used in this study. A, Avialae; B, basal archosauromorphs; C, Ceratopsia; D, Crocodylomorpha; E, Dinosauria; F, basal Ornithischia; G, Ornithopoda; H, Pterosauria; I, Sauropodmorpha; J, Theropoda; K, Thyreophora. Avialans are not included in the Dinosauria and Theropoda panels. Star symbols denote erythrosuchids. Dashed lines denote 95% confidence intervals (CIs). Regression lines and CIs from the analysis that used the *mbl*.1 time-scaled phylogeny. The theoretical isometric line ($a = 1$) is denoted by the dashed black line in each panel. Non-applicable archosauromorphs in each panel are greyed out. Taxonomic assignments for all archosauromorphs can be found in Table S1.

Fig. S2. PGLS results of log skull–length and log femur–length for each assigned archosauromorph category that produced different scaling relationships after using the *mbl*.1 and *cal3* time-scaled phylogenies. A, avialans; B, bipedal-quadruped archosauromorphs; C, terrestrial basal archosauromorph carnivores. In all panels the *cal3* regression line is denoted by a green solid line and the *mbl*.1 regression lines in panels A–C are denoted by a blue, yellow and orange solid line respectively. Dashed lines denote 95% confidence intervals (CIs). The theoretical isometric line ($a = 1$) is denoted by the dashed black line in each panel. Non-applicable archosauromorphs in each panel are greyed out. PGLS regression results can be found in Table S5.

Fig. S3. PGLS results of log skull–length and log femur–length for: A, Archosauromorpha; B, Dinosauria that include and exclude sauropodomorphs. In both panels the sauropodomorph-excluded regression line is denoted by a scarlet solid line and the sauropodomorph-included regression lines in panels A and B are denoted by a grey and blue solid line respectively. Dashed lines denote 95% confidence intervals (CIs). The theoretical isometric line ($a = 1$) is denoted by the dashed black line in each panel. Non-applicable archosauromorphs in each panel are greyed out. PGLS regression results can be found in Table S5.

Fig. S4. PGLS results of log skull–length and log femur–length for each assigned locomotory mode of extinct archosauromorphs. A, bipedal; B, bipedal-flying; C, bipedal-quadruped; D, quadrupedal. Dashed lines denote 95% confidence intervals (CIs). Regression lines and CIs from the analysis that used the *mbl*.1 time-scaled phylogeny. The theoretical isometric line ($a = 1$) is shown as a dashed black line in each panel. Non-applicable archosauromorphs in each panel are greyed out. Locomotory assignments for all archosauromorphs can be found in Table S1.

Fig. S5. PGLS results of log skull–length and log femur–length for each assigned biotope of extinct archosauromorphs. A, aerial; B, aquatic; C, terrestrial. Dashed lines denote 95% confidence intervals (CIs). Regression lines and CIs from the analysis that used the *mbl*.1 time-scaled phylogeny. The theoretical isometric line ($a = 1$) is denoted by the dashed black line in each panel. Non-applicable archosauromorphs in each panel are greyed out. Biotope assignments for all archosauromorphs can be found in Table S1.

Fig. S6. Ancestral character-state reconstructions of log skull–length/log femur–length ratio evolution for 223 archosauromorphs from mapping ratios onto time-calibrated supertrees with label numbers of all 222 nodes. A, reconstruction using the *mbl*.1 dating method. B, reconstruction using the *cal3* dating method. Ancestral node estimates, along with the variance and upper and lower 95% confidence intervals for both trees can be found in Table S6.

Table S1. Skull and femur length data of studied archosauromorphs with taxonomy, diet, locomotion and biotope assignments.

Table S2. First and last appearance data (in millions of years) of archosauromorphs used to time-scale the supertree used in our analyses.

Table S3. Phylogenetic signal results, using Pagel's lambda, of archosauromorph log skull-length/log femur-length ratio from the 40 randomly resolved, time-calibrated trees used for the model fitting analysis.

Table S4. Phylogenetic generalized least squares regression and predictor model fitting results of all 15 predictor models on archosauromorph log skull-length and log femur-length from 40 randomly resolved, time-calibrated trees.

Table S5. Phylogenetic generalized least squares regression results of archosauromorph log skull-length and log femur-length from subsets according to: taxonomic group; diet; locomotory mode; biotope; terrestrial basal archosauromorph carnivores and terrestrial dinosaur carnivores.

Table S6. Estimated ancestral archosauromorph log skull-length/log femur-length ratios for selected nodes from the *mbl*.1 and *cal3* time-calibrated trees.

Appendix S1. Nexus file for undated archosauromorph tree.

Appendix S2. Example R code.

Appendix S3. *cal3* trees (taxa dropped, 20 trees).

Appendix S4. *mbl*.1 trees (taxa dropped, 20 trees).

REFERENCES

ANDRES, B., CLARK, J. and XU, X. 2014. The earliest pterodactyloid and the origin of the group. *Current Biology*, **24**, 1011–1016.

ARBOUR, J. H., CURTIS, A. A. and SANTANA, S. E. 2019. Signatures of echolocation and dietary ecology in the adaptive radiation evolution of skull shape in bats. *Nature Communications*, **10**, 2036.

BACZKO, M. B. VON 2018. Rediscovered cranial material of *Venaticosuchus rusconii* enables the first jaw biomechanics in Ornithosuchidae (Archosauria: Pseudosuchia). *Ameghiniana*, **55**, 365–379.

BAPST, D. W. 2012. paleotree: an R package for paleontological and phylogenetic analyses of evolution. *Methods in Ecology & Evolution*, **3**, 803–807.

BAPST, D. W. 2013. A stochastic rate-calibrated method for time-scaling phylogenies of fossil taxa. *Methods in Ecology & Evolution*, **4**, 724–733.

BAPST, D. W. and HOPKINS, M. J. 2017. Comparing *cal3* and other a posteriori time-scaling approaches in a case study with the pterocephaliid trilobites. *Paleobiology*, **43**, 49–67.

BARON, M. G. 2017. *Pisanosaurus mertii* and the Triassic ornithischian crisis: could phylogeny offer a solution? *Historical Biology*, **31**, 967–981.

BARRETT, P. M. 2014. Paleobiology of herbivorous dinosaurs. *Annual Review of Earth & Planetary Sciences*, **42**, 207–230.

BARRETT, P. M. and MAIDMENT, S. C. R. 2017. The evolution of ornithischian quadrupedality. *Journal of Iberian Geology*, **43**, 363–377.

BELL, E., ANDRES, B. and GOSWAMI, A. 2011. Integration and dissociation of limb elements in flying vertebrates: a comparison of pterosaurs, birds and bats. *Journal of Evolutionary Biology*, **24**, 2586–2599.

BENNETT, S. C. 2007. A second specimen of the pterosaur *Anurognathus ammoni*. *Paläontologische Zeitschrift*, **81**, 376–398.

BENSON, R. B. J. and CHOINIERE, J. N. 2013. Rates of dinosaur limb evolution provide evidence for exceptional radiation in Mesozoic birds. *Proceedings of the Royal Society B*, **280**, 20131780.

BENSON, R. B. J., CAMPIONE, N. E., CARRANO, M. T., MANNION, P. D., SULLIVAN, C., UPCHURCH, P. and EVANS, D. C. 2014. Rates of dinosaur body mass evolution indicate 170 million years of sustained ecological innovation on the avian stem lineage. *PLoS Biology*, **12**, e1001896.

BENSON, R. B. J., HUNT, G., CARRANO, M. T. and CAMPIONE, N. E. 2018. Cope's rule and the adaptive landscape of dinosaur body size evolution. *Palaeontology*, **61**, 13–48.

BENTON, M. J. 1999. *Scleromochlus taylori* and the origin of dinosaurs and pterosaurs. *Philosophical Transactions of the Royal Society B*, **354**, 1423–1446.

BENTON, M. J. 2004. Origin and relationships of Dinosauria. 7–19. *In* WEISHAMPEL, D. B., DODSON, P. and OSMÓLSKA, H. (eds). *The Dinosauria*. Second edition. University of California Press.

BESTWICK, J., UNWIN, D. M., BUTLER, R. J., HENDERSON, D. M. and PURNELL, M. A. 2018. Pterosaur dietary hypotheses: a review of ideas and approaches. *Biological Reviews*, **93**, 2021–2048.

BESTWICK, J., UNWIN, D. M., BUTLER, R. J. and PURNELL, M. A. 2020. Dietary diversity and evolution of the earliest flying vertebrates revealed by dental microwear texture analysis. *Nature Communications*, **11**, 5293.

BHULLAR, B.-A. S., MARUGÁN-LOBÓN, J., RACIMO, F., BEVER, G. S., ROWE, T. B., NORELL, M. A. and ABZHANOV, A. 2012. Birds have paedomorphic dinosaur skulls. *Nature*, **487**, 223–226.

BIEWENER, A. A. 2005. Biomechanical consequences of scaling. *Journal of Experimental Biology*, **208**, 1665–1676.

BONAPARTE, J. F., NOVAS, F. E. and CORIA, R. A. 1990. *Carnotaurus sastrei* Bonaparte, the horned, lightly built carnosaur from the middle Cretaceous of Patagonia. *Natural History Museum of Los Angeles County*, **416**, 1–42.

BRIGHT, J. A., MARUGÁN-LOBÓN, J., COBB, S. N. and RAYFIELD, E. J. 2016. The shapes of bird beaks are highly controlled by non-dietary factors. *Proceedings of the National Academy of Sciences*, **113**, 5352–5357.

BRITT, B. B., DALLA VECCHIA, F. M., CHURE, D. J., ENGELMANN, G. F., WHITLING, M. F. and SCHEETZ, R. D. 2018. *Caelestiventus hanseni* gen. et sp. nov. extends the desert-dwelling pterosaur record back 65 million years. *Nature Ecology & Evolution*, **2**, 1386–1392.

BROWN, E. E., BUTLER, R. J., EZCURRA, M. D., BHULLAR, B.-A. S. and LAUTENSCHLAGER, S. 2020. Endocranial anatomy and life habits of the early Triassic archosauriform *Proterosuchus fergusi*. *Palaeontology*, **63**, 255–282.

BRUSATTE, S. L., BENTON, M. J., DESOJO, J. B. and LANGER, M. C. 2010*a*. The higher-level phylogeny of Archosauria (Tetrapoda: Diapsida). *Journal of Systematic Palaeontology*, **8**, 3–47.

BRUSATTE, S. L., NESBITT, S. J., IRMIS, R. B., BUT-LER, R. J., BENTON, M. J. and NORELL, M. A. 2010b. The origin and early radiation of dinosaurs. *Earth-Science Reviews*, **101**, 68–100.

BRUSATTE, S. L., SAKAMOTO, M., MONTANARI, S. and HARCOURT SMITH, W. E. H. 2012. The evolution of cranial form and function in theropod dinosaurs: insights from geometric morphometrics. *Journal of Evolutionary Biology*, **25**, 365–377.

BRUSATTE, S. L., LLOYD, G. T., WANG, S. C. and NORELL, M. A. 2014. Gradual assembly of avian body plan culminated in rapid rates of evolution across the dinosaur-bird transition. *Current Biology*, **24**, 2386–2392.

BUTLER, R. J., SENNIKOV, A. G., DUNNE, E. M., EZCURRA, M. D., HEDRICK, B. P., MAIDMENT, S. C. R., MEADE, L. E., RAVEN, T. J. and GOWER, D. J. 2019. Cranial anatomy and taxonomy of the erythrosuchid archosauriform 'Vjushkovia triplicostata' Huene, 1960, from the Early Triassic of European Russia. *Royal Society Open Science*, **6**, 191289.

BUTTON, D. J. and ZANNO, L. E. 2020. Repeated evolution and divergent modes of herbivory in non-avian dinosaurs. *Current Biology*, **30**, 158–168.

CABREIRA, S. F., KELLNER, A. W. A., DIAS-DA-SILVA, S., DA SILVA, L. R., BRONZATI, M., DE ALMEIDA MARSOLA, J. C., MÜLLER, R. T., DE SOUZA BITTENCOURT, J., BATISTA, B. J., RAUGUST, T., CARRILHO, R., BRODT, A. and LANGER, M. C. 2016. A unique dinosauromorph assemblage reveals dinosaur ancestral anatomy and diet. *Current Biology*, **26**, 3090–3095.

CAMPIONE, N. E. and EVANS, D. C. 2012. A universal scaling relationship between body mass and proximal limb bone dimensions in quadrupedal terrestrial tetrapods. *BMC Biology*, **10**, 60.

CAMPIONE, N. E., EVANS, D. C., BROWN, C. M. and CARRANO, M. T. 2014. Body mass estimation in non-avian bipeds using a theoretical conversion to quadrupedal stylopodial proportions. *Methods in Ecology & Evolution*, **5**, 913–923.

CANALE, J. I., SCANFERLA, C. A., AGNOLIN, F. L. and NOVAS, F. E. 2009. New carnivorous dinosaur from the Late Cretaceous of NW Patagonia and the evolution of abelisaurid theropods. *Naturwissenschaften*, **96**, 409–414.

CARDINI, A. 2019. Craniofacial allometry is a rule in evolutionary radiations of placentals. *Evolutionary Biology*, **46**, 239–248.

CARDINI, A. and POLLY, P. D. 2013. Larger mammals have longer faces because of size-related constraints on skull form. *Nature Communications*, **4**, 2458.

CARDINI, A., POLLY, D., DAWSON, R. and MILNE, N. 2015. Why the long face? Kangaroos and wallabies follow the same 'rule' of cranial evolutionary allometry (CREA) as placentals. *Evolutionary Biology*, **42**, 169–176.

CARRANO, M. T. 2006. Body size evolution in the Dinosauria. 225–268. *In* CARRANO, M. T., BLOB, R. W., GAUDIN, T. J. and WIBLE, J. R. (eds). *Amniote paleobiology: Perspectives on the evolution of mammals, birds, and reptiles*. University of Chicago Press.

CASHMORE, D. D., MANNION, P. D., UPCHURCH, P. and BUTLER, R. J. 2020. Ten more years of discovery: revisiting the quality of the sauropodomorph dinosaur fossil record. *Palaeontology*, **63**, 951–978.

CHATTERJEE, S. 1985. *Postosuchus*, a new thecodontian reptile from the Triassic of Texas and the origin of tyrannosaurs. *Philosophical Transactions of the Royal Society B*, **309**, 395–460.

CHRISTIANSEN, P. 1999. On the head size of sauropodomorph dinosaurs: implications for ecology and physiology. *Historical Biology*, **13**, 269–297.

DA SILVA, F. O., FABRE, A.-C., SAVRIAMA, Y., OLLONEN, J., MAHLOW, K., HERREL, A., MÜLLER, J. and DI-POÏ, N. 2018. The ecological origins of snake as revealed by skull evolution. *Nature Communications*, **9**, 376.

DALLA VECCHIA, F. M. 2013. Triassic pterosaurs. 119–155. *In* NESBITT, S. J., DESOJO, J. B. and IRMIS, R. B. (eds). *Anatomy, phylogeny and palaeobiology of early archosaurs and their kin*. Geological Society, London, Special Publications, **379**.

DEAN, C. D., MANNION, P. D. and BUTLER, R. J. 2016. Preservational bias controls the fossil record of pterosaurs. *Palaeontology*, **59**, 225–247.

DECECCHI, T. A. and LARSSON, H. C. E. 2013. Body and limb size dissociation at the origin of birds: uncoupling allometric constraints across a macroevolutionary transition. *Evolution*, **67**, 2741–2752.

DELCOURT, R. and GRILLO, O. N. 2018. Tyrannosauroids from the Southern Hemisphere: implications for biogeography, evolution, and taxonomy. *Palaeogeography, Palaeoclimatology, Palaeoecology*, **511**, 379–387.

DESOJO, J. B., BACZKO, M. B. VON and RAUHUT, O. W. M. 2020a. Anatomy, taxonomy and phylogenetic relationships of *Prestosuchus chiniquensis* (Archosauria: Pseudosuchia) from the original collection of von Huene, Middle-Late Triassic of southern Brazil. *Palaeontologia Electronica*, **23**, a04.

DESOJO, J. B., FIORELLI, L. E., EZCURRA, M. D., MARTINELLI, A. G., RAMEZANI, J., DA ROSA, A. A. S., BACZKO, M. B. VON, TROTTEYN, M. J., MONTEFELTRO, F. C., EZPELETA, M. and LANGER, M. C. 2020b. The Late Triassic Ischigualasto Formation at Cerro las Lajas (La Pioja, Argentina): fossil tetrapods, high-resolution chronostratigraphy, and faunal correlations. *Scientific Reports*, **10**, 1–34.

DILKES, D. W. 1998. The Early Triassic rhynchosaur *Mesosuchus browni* and the interrelationships of basal archosauromorph reptiles. *Philosophical Transactions of the Royal Society B*, **353**, 501–541.

ERICKSON, G. M., GIGNAC, P. M., STEPPAN, S. J., LAPPIN, A. K., VLIET, K. A., BRUEGGEN, J. D., INOUYE, B. D., KLEDZIK, D. and WEBB, G. J. 2012. Insights into the ecology and evolutionary success of crocodilians revealed through bite-force and tooth-pressure experimentation. *PLoS One*, **7**, e31781.

EZCURRA, M. D. 2016. The phylogenetic relationships of basal archosauromorphs, with an emphasis on the systematics of proterosuchian archosauriforms. *PeerJ*, **4**, e1778.

EZCURRA, M. D. and BUTLER, R. J. 2018. The rise of ruling reptiles and ecosystem recovery from the Permo-Triassic mass extinction. *Proceedings of the Royal Society B*, **285**, 20180361.

EZCURRA, M. D., LECUONA, A. and MARTINELLI, A. 2010. A new basal archosauriform diapsid from the Lower Triassic of Argentina. *Journal of Vertebrate Paleontology*, 30, 1433–1450.

EZCURRA, M. D., BUTLER, R. J. and GOWER, D. J. 2013. 'Proterosuchia': the origin and early history of Archosauriformes. 9–33. *In* NESBITT, S. J., DESOJO, J. B. and IRMIS, R. B. (eds). *Anatomy, phylogeny and palaeobiology of early archosaurs and their kin*. Geological Society, London, Special Publications, 379.

EZCURRA, M. D., NESBITT, S. J., BRONZATI, M., DALLA VECCHIA, F. M., AGNOLIN, F. L., BENSON, R. B. J., EGLI, F. B., CABREIRA, S. F., EVERS, S. W., GENTIL, A. R., IRMIS, R. B., MARTINELLI, A. G., NOVAS, F. E., DA SILVA, L. R., SMITH, N. D., STOCKER, M. R., TURNER, A. H. and LANGER, M. C. 2020a. Enigmatic dinosaur precursors bridge the gap to the origin of Pterosauria. *Nature*, 588, 445–449.

EZCURRA, M. D., JONES, A. S., GENTIL, A. R. and BUTLER, R. J. 2020b. Early archosauromorphs: the crocodile and dinosaur precursors. 175–185. *In* ALDERTON, D. and ELIAS, S. A. (eds). *Encyclopedia of geology*. Second edition. Academic Press.

EZCURRA, M. D., BANDYOPADHYAY, S. and GOWER, D. J. 2021. A new erythrosuchid archosauriform from the middle Triassic Yerrapalli Formation of South-Central India. *Ameghiniana*, 58, 132–168.

FABBRI, M., NAVALÓN, G., MONGIARDINO KOCH, N., HANSON, M., PETERMANN, H. and BHULLAR, B.-A. S. 2021. A shift in ontogenetic timing produced the unique sauropod skull. *Evolution*, 75, 819–831.

FABRE, A.-C., BICKFORD, D., SEGALL, M. and HERREL, A. 2016. The impact of diet, habitat use and behaviour on head shape evolution in homalopsid snakes. *Biological Journal of the Linnean Society*, 118, 634–647.

FELICE, R. N., POL, D. and GOSWAMI, A. 2021. Complex macroevolutionary dynamics underly the evolution of the crocodyliform skull. *Proceedings of the Royal Society B*, 288, 20210919.

FERRY-GRAHAM, L. A., BOLNICK, D. I. and WAINWRIGHT, P. C. 2002. Using functional morphology to examine the ecology and evolution of specialization. *Integrative & Comparative Biology*, 42, 265–277.

FIGUEIRIDO, B., SERRANO-ALARCÓN, F. J., SLATER, G. J. and PALMQVIST, P. 2010. Shape at the cross-roads: homoplasy and history in the evolution of the carnivoran skull towards herbivory. *Journal of Experimental Biology*, 23, 2579–2594.

FISHER, D. C. 1985. Evolutionary morphology: beyond the analogous, the anecdotal and the ad hoc. *Paleobiology*, 11, 120–138.

FOTH, C., BONA, P. and DESOJO, J. B. 2015. Intraspecific variation in the skull morphology of the black caiman *Melanosuchus niger* (Alligatoridae, Caimaninae). *Acta Zoologica*, 96, 1–13.

FOTH, C., EZCURRA, M. D., SOOKIAS, R. B., BRUSATTE, S. L. and BUTLER, R. J. 2016a. Unappreciated diversification of stem archosaurs during the Middle Triassic predated the dominance of dinosaurs. *BMC Evolutionary Biology*, 16, 188.

FOTH, C., HENDRICK, B. P. and EZCURRA, M. D. 2016b. Cranial ontogenetic variation in early saurischians and the role of heterochrony in the diversification of predatory dinosaurs. *PeerJ*, 4, e1589.

FOTH, C., SOOKIAS, R. B. and EZCURRA, M. D. 2021. Rapid initial morphospace expansion and delayed morphological disparity peak in the first 100 million years of the archosauromorph evolutionary expansion. *Frontiers in Earth Science*, 9, 723973.

FUNSTON, G. F., MENDONCA, S. E., CURRIE, P. J. and BARSBOLD, R. 2018. Oviraptorosaur anatomy, diversity and ecology in the Nemegt Basin. *Palaeogeography, Palaeoclimatology, Palaeoecology*, 494, 101–120.

GALATIUS, A., RACICOT, R., McGOWEN, M. and OLSEN, M. T. 2020. Evolution and diversification of delphinid skull shapes. *iScience*, 23, 101543.

GALTON, M. P. and UPCHURCH, P. 2004. Prosauropoda. 232–258. *In* WEISHAMPEL, D. B., DODSON, P. and OSMÓLSKA, H. (eds). *The Dinosauria*. Second edition. University of California Press.

GODOY, P. L., BENSON, R. B. J., BRONZATI, M. and BUTLER, R. J. 2019. The multi-peak adaptive landscape of crocodylomorph body size evolution. *BMC Evolutionary Biology*, 19, 167.

GOULD, S. J. and LEWONTIN, R. C. 1979. The spandrels of San Marco and the Panglossian paradigm: a critique of the adaptationist programme. *Proceedings of the Royal Society B*, 205, 581–598.

GRIGG, G. and KIRSHNER, D. 2015. *Biology and evolution of crocodylians*. Cornell University Press.

HARTMAN, S., MORTIMER, M., WAHL, W. R., LOMAX, D. R., LIPPINCOTT, J. and LOVELACE, D. M. 2019. A new paravian dinosaur from the Late Jurassic of North America supports a late acquisition of avian flight. *PeerJ*, 7, e7247.

HENDERSON, D. M. 1999. Estimating the masses and centers of mass of extinct animals by 3-D mathematical slicing. *Paleobiology*, 25, 88–106.

HENDERSON, D. M. 2018. A buoyancy, balance and stability challenge to the hypothesis of a semi-aquatic *Spinosaurus* Stromer, 1915 (Dinosauria: Theropoda). *PeerJ*, 6, e5409.

HENDRICKX, C. and MATEUS, O. 2014. *Torvosaurus gurneyi* n. sp., the largest terrestrial predator from Europe, and a proposed terminology of the maxilla anatomy in nonavian theropods. *PLoS One*, 9, e88905.

HOLLIDAY, J. A. and STEPPAN, S. J. 2004. Evolution of hypercarnivory: the effect of specialization on morphological and taxonomic diversity. *Paleobiology*, 30, 108–128.

HOLTZ, T. R. Jr 2004. Tyrannosauroidea. 111–136. *In* WEISHAMPEL, D. B., DODSON, P. and OSMÓLSKA, H. (eds). *The Dinosauria*. Second edition. University of California Press.

IBRAHIM, N., MAGANUCO, S., DAL SASSO, C., FABBRI, M., AUDITORE, M., BINDELLINI, G., MARTILL, D. M., ZOUHRI, S., MATTARELLI, D. A., UNWIN, D. M., WIEMANN, J., BONADONNA, D., AMANE, A., JAKUBCZAK, J., JOGER, U., LAUDER,

G. V. and PIERCE, S. E. 2020. Tail propelled aquatic locomotion in a theropod dinosaur. *Nature*, **581**, 67–70.

INGRAM, T. and MAHLER, D. L. 2013. SURFACE: detecting convergent evolution from comparative data by fitting Ornstein-Uhlenbeck models with stepwise Akaike Information Criterion. *Methods in Ecology & Evolution*, **4**, 416–425.

IRMIS, R. B., NESBITT, S. J. and SUES, H.-D. 2013. Early Crocodylomorpha. 275–302. *In* NESBITT, S. J., DESOJO, J. B. and IRMIS, R. B. (eds). *Anatomy, phylogeny and palaeobiology of early archosaurs and their kin*. Geological Society, London, Special Publications, **379**.

IRMIS, R. B., PARKER, W. G., NESBITT, S. J. and LIU, J. 2007. Early ornithischian dinosaurs: the Triassic record. *Historical Biology*, **19**, 3–22.

KECK, F., RIMET, F., BOUCHEZ, A. and FRANC, A. 2016. phylosignal: an R package to measure, test, and explore the phylogenetic signal. *Ecology & Evolution*, **6**, 2774–2780.

LAMANNA, M. C., SUES, H.-D., SCHACHNER, E. R. and LYSON, T. R. 2014. A new large-bodied oviraptorosaurian theropod dinosaur from the Latest Cretaceous of western North America. *PLoS One*, **9**, e92022.

LANGER, M. C. 2004. Basal Saurischia. 25–46. *In* WEISHAMPEL, D. B., DODSON, P. and OSMÓLSKA, H. (eds). *The Dinosauria*. Second edition. University of California Press.

LANGER, M. C., EZCURRA, M. D., BITTENCOURT, J. S. and NOVAS, F. E. 2010. The origin and evolution of early dinosaurs. *Biological Reviews*, **85**, 55–110.

LAURIN, M. 2004. The evolution of body size, Cope's rule and the origin of amniotes. *Systematic Biology*, **53**, 594–622.

LAW, C. J., DURAN, E., HUNG, N., RICHARDS, E., SANTILLAN, I. and MEHTA, R. S. 2018. Effects of diet on cranial morphology and biting ability in musteloid mammals. *Journal of Evolutionary Biology*, **31**, 1918–1931.

LEE, Y.-N., BARSBOLD, R., CURRIE, P. J., KOBAYASHI, Y., LEE, H.-J., GODEFROIT, P., ESCUILLIÉ, F. and CHINZORIG, T. 2014a. Resolving the long-standing enigmas of a giant ornithomimosaur *Deinocheirus mirificus*. *Nature*, **515**, 257–260.

LEE, M. S. Y., CAU, A., NAISH, D. and DYKE, G. J. 2014b. Sustained miniaturization and anatomical innovation in the dinosaurian ancestors of birds. *Science*, **345**, 562–566.

LEE, H. W., ESTEVE-ALTAVA, B. and ABZHANOV, A. 2020. Evolutionary and ontogenetic changes of the anatomical organization and modularity in the skull of archosaurs. *Scientific Reports*, **10**, 1–13.

LINDE-MEDINA, M. 2016. Testing the cranial evolutionary allometric 'rule' in Galliformes. *Journal of Evolutionary Biology*, **29**, 1873–1878.

LLOYD, G. T., BAPST, D. W., FRIEDMAN, M. and DAVIS, K. E. 2016. Probabilistic divergence time estimation without branch lengths: dating the origins of dinosaurs, avian flight and crown birds. *Biology Letters*, **12**, 20160609.

LONGRICH, N. R., MARTILL, D. M. and ANDRES, B. 2018. Late Maastrichtian pterosaurs from North Africa and mass extinction of Pterosauria at the Cretaceous-Paleogene boundry. *PLoS Biology*, **16**, e2001663.

LÜ, J., UNWIN, D. M., JIN, X., LIU, Y. and JI, Q. 2010. Evidence for modular evolution in a long-tailed pterosaur

with a pterodactyloid skull. *Proceedings of the Royal Society B*, **277**, 383–389.

MAIDMENT, S. C. R., HENDERSON, D. M. and BARRETT, P. M. 2014. What drove reversions to quadrupedality in ornithischian dinosaurs? Testing hypotheses using centre of mass modelling. *Naturwissenschaften*, **101**, 989–1001.

MAIDMENT, S. C. R., SENNIKOV, A. G., EZCURRA, M. D., DUNNE, E. M., GOWER, D. J., HEDRICK, B. P., MEADE, L. E., RAVEN, T. J., PASCHCHENKO, D. I. and BUTLER, R. J. 2020. The postcranial skeleton of the erythrosuchid archosauriform *Garjainia prima* from the Early Triassic of European Russia. *Royal Society Open Science*, **7**, 201089.

MASTRANTONIO, B. M., BACZKO, M. B. VON, DESOJO, J. B. and SCHULTZ, C. L. 2019. The skull anatomy and cranial endocast of the pseudosuchid archosaur *Prestosuchus chiniquensis* from the Triassic of Brazil. *Acta Palaeontologica Polonica*, **64**, 171–198.

MAZETTA, G. V., CISILINO, A. P., BLANCO, R. E. and CALVO, N. 2009. Cranial mechanics and functional interpretation of the horned carnivorous dinosaur *Carnotaurus sastrei*. *Journal of Vertebrate Paleontology*, **29**, 822–830.

McCURRY, M. R., MAHONY, M., CLAUSEN, P. D., QUAYLE, M. R., WALMSLEY, C. W., JESSOP, T. S., WROE, S., RICHARDS, H. and McHENRY, C. R. 2015. The relationship between cranial structure, biomechanical performance and ecological diversity in varanoid lizards. *PLoS One*, **10**, e0130625.

McCURRY, M. R., FITZGERALD, E. M. G., EVANS, A. R., ADAMS, J. W. and McHENRY, C. R. 2017. Skull shape reflects prey size niche in toothed whales. *Biological Journal of the Linnean Society*, **121**, 936–946.

McDONALD, A. T., GATES, T. A., ZANNO, L. E. and MAKOVICKY, P. J. 2017. Anatomy, taphonomy, and phylogenetic implications of a new specimen of *Eolambia caroljonesa* (Dinosauria: Ornithopoda) from the Cedar Mountain Formation, Utah, USA. *PLoS One*, **12**, e0176896.

MELSTROM, K. M. and IRMIS, R. B. 2019. Repeated evolution of herbivorous crocodyliforms during the age of dinosaurs. *Current Biology*, **29**, 2389–2395.

MILLER, C. V. and PITTMAN, M. 2021. The diet of early birds based on modern and fossil evidence and a new framework for its reconstruction. *Biological Reviews*, **96**, 2058–2112.

MOLINA-VENEGAS, R. and RODRÍGUEZ, M. A. 2017. Revisiting phylogenetic signal; strong or negligible impacts of polytomies and branch length information? *BMC Ecology & Evolution*, **17**, 53.

MOLNAR, J. L., PIERCE, S. E., BHULLAR, B.-A. S., TURNER, A. H. and HUTCHINSON, J. R. 2015. Morphological and functional changes in the vertebral column with increasing aquatic adaptation in crocodylomorphs. *Royal Society Open Science*, **2**, 150439.

MONTEFELTRO, F. C., LAUTENCHLAGER, S., GODOY, P. L., FERREIRA, G. S. and BUTLER, R. J. 2020. A unique predator in a unique ecosystem: modelling the apex predator within a Late Cretaceous crocodyliform-dominated fauna from Brazil. *Journal of Anatomy*, **237**, 323–333.

MONTGOMERY, S. H., GEISLER, J. H., McGOWEN, M. R., FOX, C., MARINO, L. and GATESY, J. 2013. The

evolutionary history of cetacean brain and body size. *Evolution*, **67**, 3339–3353.

MORRIS, Z. S., VILET, K. A., ABZHANOV, A. and PIERCE, S. E. 2019. Heterochronic shifts and conserved embryonic shape underlie crocodylian craniofacial disparity and convergence. *Proceedings of the Royal Society B*, **286**, 20182389.

MÜLLER, R. T. and GARCIA, M. S. 2020. A paraphyletic 'Silesauridae' as an alternative hypothesis for the initial radiation of ornithischian dinosaurs. *Biology Letters*, **16**, 20200417.

MÜLLER, R. T., VON BACZKO, M. B., DESOJO, J. B. and NESBITT, S. J. 2020. The first ornithosuchid from Brazil and its macroevolutionary and phylogenetic implications for Late Triassic faunas in Gondwana. *Acta Palaeontologica Polonica*, **65**, 1–10.

MÜNKEMÜLLER, T., LAVERGNE, S., BZEZNIK, B., DRAY, S., JOMBART, T., SCHIFFERS, K. and THUILLER, W. 2012. How to measure and test phylogenetic signal. *Methods in Ecology & Evolution*, **3**, 743–756.

NAISH, D., CAU, A., HOLTZ, T. R. Jr, FABBRI, M. and GAUTHIER, J. A. 2020. Theropoda O. C. Marsh 1881 [D. Naish, A. Cau, T. R. Holtz, Jr., M. Fabbri, and J. A. Gauthier], converted clade name. 1236–1246. *In* DE QUEIROZ, K., CANTINO, P. D. and GAUTHIER, J. A. (eds). *Phylonyms: A companion to the PhyloCode*. CRC Press.

NEBREDA, S. M., FERNÁNDEZ, M. H. and MARUGÁN-LOBÓN, J. 2021. 'Dinosaur-bird' macroevolution, locomotor modules and the origins of flight. *Journal of Iberian Geology*, **47**, 565–574.

NESBITT, S. J. 2011. The early evolution of archosaurs: relationships and the origin of major clades. *Bulletin of the American Museum of Natural History*, **352**, 1–292.

NESBITT, S. J. and DESOJO, J. B. 2017. The osetology and phylogenetic position of *Luperosuchus fractus* (Archosauria: Loricata) from the latest Middle Triassic or earliest Late Triassic of Argentina. *Ameghiniana*, **54**, 261–282.

NESBITT, S. J., BRUSATTE, S. L., DESOJO, J. B., LIPARINI, A., DE FRANÇA, M. A. G., WEINBAUM, J. C. and GOWER, D. J. 2013. Rauisuchia. 241–274. *In* NESBITT, S. J., DESOJO, J. B. and IRMIS, R. B. (eds). *Anatomy, phylogeny and palaeobiology of early archosaurs and their kin*. Geological Society, London, Special Publications, **379**.

NORMAN, D. B., SUES, H.-D., WITMER, L. M. and CORIA, R. A. 2004*a*. Basal Ornithopoda. 393–412. *In* WEISHAMPEL, D. B., DODSON, P. and OSMÓLSKA, H. (eds). *The Dinosauria*. Second edition. University of California Press.

NORMAN, D. B., WITMER, L. M. and WEISHAMPEL, D. B. 2004*b*. Basal Thyreophora. 335–342. *In* WEISHAMPEL, D. B., DODSON, P. and OSMÓLSKA, H. (eds). *The Dinosauria*. Second edition. University of California Press.

NOVAS, F. E., AGNOLIN, F. L., EZCURRA, M. D., MÜLLER, R. T., MARTINELLI, A. G. and LANGER, M. C. 2021. Review of the fossil record of early dinosaurs from South America, and its phylogenetic implications. *Journal of South American Earth Sciences*, **110**, 103341.

NOVAS, F. E., AGNOLIN, F. L., EZCURRA, M. D., PORFIRI, J. and CANALE, J. I. 2013. Evolution of the carnivorous dinosaurs during the Cretaceous: the evidence from Patagonia. *Cretaceous Research*, **45**, 174–215.

O'BRIEN, H. D., LYNCH, L. M., VILET, K. A., BRUEGGEN, J., ERICKSON, G. M. and GIGNAC, P. M. 2019. Crocodylian head width allometry and phylogenetic prediction of body size in extinct crocodliforms. *Integrative Organismal Biology*, **1**, obz006.

OPENSHAW, G. H. and KEOGH, J. S. 2014. Head shape evolution in monitor lizards (*Varanus*): interactions between extreme size disparity, phylogeny and ecology. *Journal of Experimental Biology*, **27**, 363–373.

ŐSI, A. 2014. The evolution of jaw mechanism and dental function in heterodont crocodyliforms. *Historical Biology*, **26**, 279–414.

OSTROM, J. H. 1966. Functional morphology and evolution of the ceratopsian dinosaurs. *Evolution*, **20**, 290–308.

PARKER, W. G., NESBITT, S. J., IRMIS, R. B., MARTZ, J. W., MARSH, A. D., BROWN, M. A. and STOCKER, M. R. 2021. Osteology and relationships of *Revueltosaurus callenderi* (Archosauria: Suchia) from the Upper Triassic (Norian) Chinle Formation of Petrified Forest National Park, Arizona, United States. *The Anatomical Record*, published online 29 Spetember. https://doi.org/10.1002/ar.24757

PEI, R., PITTMAN, M., GOLOBOFF, P. A., DECECCHI, A., HABIB, M. B., KAYE, T. G., LARSSON, H. C. E., NORELL, M. A., BRUSATTE, S. L. and XU, X. 2020. Potential for powered flight neared by most close avialan relatives, but few crossed its thresholds. *Current Biology*, **30**, 4033–4046.

PINHEIRO, J., BATES, D., DEBROY, S. and SARKAR, D. 2018. nlme: linear and nonlinear mixed effects models. R package 3.1-137. https://CRAN.R-project.org/package=nlme

POL, D. and RAUHUT, O. W. M. 2012. A Middle Jurassic abelisaurid from Patagonia and the early diversification of theropod dinosaurs. *Proceedings of the Royal Society B*, **279**, 3170–3175.

POL, D., LEARDI, J. M., LECUNA, A. and KRAUSE, M. 2012. Postcranial anatomy of *Sebecus icaeorhinus* (Crocodyliformes, Sebecidae) from the Eocene of Patagonia. *Journal of Vertebrate Paleontology*, **32**, 328–354.

PRADELLI, L. A., LEARDI, J. M. and EZCURRA, M. D. 2021. Body size disparity of the archosauromorph reptiles during the first 90 million years of their evolution. *Ameghiniana*, **59**, 47–77.

PUTTICK, M. N., THOMAS, G. H. and BENTON, M. J. 2014. High rates of evolution preceded the origin of birds. *Evolution*, **68**, 1497–1510.

R CORE TEAM 2018. R: a language and environment for statistical computing. R Foundation for Statistical Computing, Vienna, Austria. http://www.R-project.org/

RAUHUT, O. W. M. and POL, D. 2019. Probable basal allosauroid from the early Middle Jurassic Cañadón Asfalto Formation of Argentina highlights phylogenetic uncertainty in tetanuran theropod dinosaurs. *Scientific Reports*, **9**, 18826.

RAUHUT, O. W. M., FECHNER, R., REMES, K. and REIS, K. 2011. How to get big in the Mesozoic: the evolution of the sauropodomorph body plan. 119–149. *In* KLEIN, N., REMES, K., GEE, C. T. and SANDER, P. M. (eds).

Biology of the sauropod dinosaurs: Understanding the life of giants. Indiana University Press.

RAVEN, T. J. and MAIDMENT, S. C. R. 2017. A new phylogeny of Stegosauria (Dinosauria, Ornithischia). *Palaeontology*, **60**, 401–408.

RAYNER, J. M. V. 1988. The evolution of vertebrate flight. *Biological Journal of the Linnean Society*, **34**, 269–287.

REVELL, L. J. 2012. phytools: an R package for phylogenetic comparative biology (and other things). *Methods in Ecology & Evolution*, **3**, 217–223.

RIVERA-SYLVA, H. E., FREY, E., STINNESBECK, W., CARBOT-CHANONA, G., SANCHEZ-URIBE, I. E. and GUZMÁN-GUTIÉRREZ, J. R. 2018. Paleodiversity of Late Cretaceous Ankylosauria from Mexico and their phylogenetic significance. *Swiss Journal of Palaeontology*, **137**, 83–93.

RODRIGUES, T., JIANG, S., CHENG, X., WANG, X. and KELLNER, A. W. A. 2015. A new toothed pteranodontoid (Pterosauria, Pterodactyloidea) from the Jiufotang Formation (Lower Cretaceous, Aptian) of China and comments on *Liaoningopterus gui* Wang and Zhou, 2003. *Historical Biology*, **27**, 782–795.

SANDER, P. M., CHRISTIAN, A., CLAUSS, M., FECHNER, R., GEE, C. T., GRIEBLER, E.-M., GUNGA, H.-C., HUMMEL, J., MALLISON, H., PERRY, S. F., PREUSCHOFT, H., RAUHUT, O. W. M., REMES, K., TÜTKEN, T., WINGS, O. and WITZEL, U. 2010. Biology of the sauropod dinosaurs: the evolution of gigantism. *Biological Reviews*, **86**, 117–155.

SERENO, P. C. 2005. The logical basis of phylogenetic taxonomy. *Systematic Biology*, **54**, 595–619.

SERENO, P. C., BECK, A. L., DUTHEIL, D. B., GADO, B., LARSSON, H. C. E., LYON, G. H., MARCOT, J. D., RAUHUT, O. W. M., SADLEIR, R. W., SIDOR, C. A., VARRICCHIO, D. D., WILSON, G. P. and WILSON, J. A. 1998. A long-snouted predatory dinosaur from Africa and the evolution of spinosaurids. *Science*, **282**, 1298–1302.

SERENO, P. C., XIJIN, Z., BROWN, L. and LIN, T. 2007. New psittacosaurid highlights skull enlargement in horned dinosaurs. *Acta Palaeontologica Polonica*, **52**, 275–284.

SHATKOVSKA, O. V. and GHAZALI, M. 2021. Relative skull size as one of the factors limiting skull shape variation in passerines. *Canadian Journal of Zoology*, **99**, 1054–1066.

SLATER, G. J. and VAN VALKENBURGH, B. 2009. Allometry and performance: the evolution of skull form and function in felids. *Journal of Evolutionary Biology*, **22**, 2278–2287.

SOOKIAS, R. B., BUTLER, R. J. and BENSON, R. B. J. 2012. Rise of dinosaurs reveals major body-size transitions are driven by passive processes of trait evolution. *Proceedings of the Royal Society B*, **279**, 2180–2187.

STEPHENS, D. W., BROWN, J. S. and YDENBERG, R. C. 2007. *Foraging behaviour and ecology*. University of Chicago Press.

STOCKER, M. R. and BUTLER, R. J. 2013. Phytosauria. 91–117. *In* NESBITT, S. J., DESOJO, J. B. and IRMIS, R. B. (eds). *Anatomy, phylogeny and palaeobiology of early archosaurs and their kin*. Geological Society, London, Special Publications, **379**.

STOCKER, M. R., ZHAO, L.-J., NESBITT, S. J., WU, X.-C. and LI, C. 2017. A short-snouted, Middle Triassic phytosaur and its implications for the morphological evolution and biogeography of Phytosauria. *Scientific Reports*, **7**, 46028.

STUBBS, T. L., PIERCE, S. E., RAYFIELD, E. J. and ANDERSON, P. S. 2013. Morphological and biomechanical disparity of crocodile-line archosaurs following the end-Triassic extinction. *Proceedings of the Royal Society B*, **280**, 20131940.

STUBBS, T. L., PIERCE, S. E., ELSER, A., ANDERSON, P. S. L., RAYFIELD, E. J. and BENTON, M. J. 2021. Ecological opportunity and the rise and fall of crocodylomorph evolutionary innovation. *Proceedings of the Royal Society B*, **288**, 20210069.

SUES, H.-D., FREY, E., MARTILL, D. M. and SCOTT, D. M. 2002. *Irritator challengeri*, a spinosaurid (Dinosauria: Theropoda) from the Lower Cretaceous of Brazil. *Journal of Vertebrate Paleontology*, **22**, 535–547.

TAMAGNINI, D., MELORO, C. and CARDINI, A. 2017. Anyone with a long-face? Craniofacial evolutionary allometry (CREA) in a family of short-faced mammals, the Felidae. *Evolutionary Biology*, **44**, 476–495.

THERRIEN, F. and HENDERSON, D. M. 2007. My theropod is bigger than yours . . . or not: estimating body size from skull length in theropods. *Journal of Vertebrate Paleontology*, **27**, 108–115.

TOKITA, M. 2015. How the pterosaur got its wings. *Biological Reviews*, **90**, 1163–1178.

TOKITA, M., YANO, W., JAMES, H. F. and ABZHANOV, A. 2016. Cranial shape evolution in adaptive radiations of birds: comparative morphometrics of Darwin's finches and Hawaiian honeycreepers. *Philosophical Transactions of the Royal Society B*, **372**, 20150481.

TROTTEYN, M. J., ARCUCCI, A. B. and RAUGUST, T. 2013. Proterochampsia: an endemic archosauriform clade from South America. 59–90. *In* NESBITT, S. J. and DESOJO, J. B. and IRMIS, R. B. (eds). *Anatomy, phylogeny and palaeobiology of early archosaurs and their kin*. Geological Society, London, Special Publications, **379**.

TURNER, A. H. and NESBITT, S. J. 2013. Body size evolution during the Triassic archosauriform radiation. 573–597. *In* NESBITT, S. J., DESOJO, J. B. and IRMIS, R. B. (eds). *Anatomy, phylogeny and palaeobiology of early archosaurs and their kin*. Geological Society, London, Special Publications, **379**.

TURNER, A. H., MAKOVICKY, P. J. and NORELL, M. A. 2012. A review of dromaeosaurid systematics and paravian phylogeny. *Bulletin of the American Museum of Natural History*, **371**, 1–206.

TYKOSKI, R. S. and ROWE, T. 2004. Ceratosauria. 47–70. *In* WEISHAMPEL, D. B., DODSON, P. and OSMÓLSKA, H. (eds). *The Dinosauria*. Second edition. University of California Press.

VANBUREN, C. S., CAMPIONE, N. E. and EVANS, D. C. 2015. Head size, weaponry, and cervical adaptation: testing craniocervical evolutionary hypotheses in Ceratopsia. *Evolution*, **69**, 1728–1744.

VENDITTI, C., BAKER, J., BENTON, M. J., MEADE, L. E. and HUMPHRIES, S. 2020. 150 million years of sustained increase in pterosaur flight efficiency. *Nature*, **379**, 83–86.

WALMSLEY, C. W., SMITS, P. D., QUAYLE, M. R., McCURRY, M. R., RICHARDS, H. S., OLDFIELD, C. C., WROE, S., CLUASEN, P. D. and McHENRY, C. R. 2013. Why the long face? The mechanics of mandibular symphysis proportions in crocodiles. *PLoS One*, **8**, e53873.

WANG, S., STIEGLER, J., AMIOT, R., WANG, X., DU, G.-H., CLARK, J. M. and XU, X. 2017. Extreme ontogenetic changes in a ceratosaurian theropod. *Current Biology*, **144**, 144–148.

WATANABE, A., FABRE, A.-C., FELICE, R. N., MAISANO, J. A., MÜLLER, J., HERREL, A. and GOSWAMI, A. 2019. Ecomorphological diversification in squamates from conserved pattern of cranial integration. *Proceedings of National Academy of Sciences*, **116**, 14688–14697.

WEINBAUM, J. C. 2011. The skull of *Postosuchus kirkpatricki* (Archosauria: Paracrocodyliformes) from the Upper Triassic of the United States. *PaleoBios*, **30**, 18–44.

WEINBAUM, J. C. 2013. Postcranial skeleton of *Postosuchus kirkpatricki* (Archosauria: Paracrocodylomorpha), from the Upper Triassic of the United States. 525–553. *In* NESBITT, S. J., DESOJO, J. B. and IRMIS, R. B. (eds). *Anatomy, phylogeny and palaeobiology of early archosaurs and their kin*. Geological Society, London, Special Publications, **379**.

WICK, S. L., LEHMAN, T. M. and BRINK, A. A. 2015. A theropod tooth assemblage from the lower Aguja Formation (early Campanian) of West Texas, and the roles of small theropod and varanoid lizard mesopredators in a tropical predator guild. *Palaeogeography, Palaeoclimatology, Palaeoecology*, **418**, 229–244.

WILBERG, E. W., TURNER, A. H. and BROCHU, C. A. 2019. Evolutionary structure and timing of major habitat shifts in Crocodylomorpha. *Scientific Reports*, **9**, 514.

WILLIAMSON, T. E. and BRUSATTE, S. L. 2016. Pachycephalosaurs (Dinosauria: Ornithischia) from the Upper Cretaceous (upper Campanian) of New Mexico: A reassessment of *Stegoceras novomexicanum*. *Cretaceous Research*, **62**, 29–43.

WITTON, M. P. 2015. Were early pterosaurs inept terrestrial locomotors? *PeerJ*, **3**, e1018.

WITTON, M. P. and HABIB, M. B. 2010. On the size and flight diversity of giant pterosaurs, the use of birds as pterosaur analogues and comments on pterosaur flightlessness. *PLoS One*, **5**, e13982.

WYND, B. M., NESBITT, S. J., STOCKER, M. R. and HECKERT, A. B. 2019. A detailed description of *Rugarhynchos sixilensis*, gen. et comb. nov. (Archosauriformes, Proterochampsia), and cranial convergence in snout elongation across stem and crown archosaurs. *Journal of Vertebrate Paleontology*, **39**, e1748042.

XING, H. and XING, X. 2014. Comparative osteology and phylogenetic relationship of *Edmontosaurus* and *Shatungosaurus* (Dinosauria: Hadrosaurida) from the Upper Cretaceous of North America and East Asia. *Acta Geologica Sinica*, **88**, 1801–1840.

XU, X., SULLIVAN, C., PITTMAN, M., CHOINIERE, J. N., HONE, D., UPCHURCH, P., TAN, Q., XIAO, D., TAN, L. and HAN, F. 2010. A monodactyl nonavian dinosaur and the complex evolution of the alvarezoid hand. *Proceedings of National Academy of Sciences*, **108**, 2338–2342.

YOU, H. and DODSON, P. 2004. Basal Ceratopsia. 478–493. *In* WEISHAMPEL, D. B., DODSON, P. and OSMÓLSKA, H. (eds). *The Dinosauria*. Second edition. University of California Press.

YOUNG, M. T., BRUSATTE, S. L., RUTA, M., and DE ANDRADE, M. B. 2010. The evolution of Metriorhynchoidea (Mesoeucrocodylia, Thalattosuchia): an integrated approach using geometric morphometrics, analysis of disparity, and biomechanics. *Zoological Journal of the Linnean Society*, **158**, 801–859.

ZANNO, L. E. and MAKOVICKY, P. J. 2013. No evidence for directional evolution of body mass in herbivorous theropod dinosaurs. *Proceedings of the Royal Society B*, **280**, 20122526.